Earth-Science Reviews 92 (2009) 35–51

Contents lists available at ScienceDirect

Earth-Science Reviews

journal homepage: www.elsevier.com/locate/earscirev

Effects of peat compaction on delta evolution: A review on processes, responses, measuring and modeling

S. van Asselen *, E. Stouthamer, Th.W.J. van Asch

Department of Physical Geography, Faculty of Geosciences, Utrecht University, P.O. Box 80.115, 3508 TC Utrecht, The Netherlands

ARTICLE INFO

Article history:
Received 27 March 2008
Accepted 2 November 2008
Available online 19 November 2008

Keywords:
peat compaction
delta evolution
quantifying compaction
numerical compaction models

ABSTRACT

Peat is most compressible of all natural soils. Compaction of peat layers potentially leads to substantial amounts of land subsidence. Peat is common in many distal parts of Holocene deltas, which are often densely populated. It is known that land subsidence due to peat compaction may have serious societal implications in such areas, as it may cause damage to construction works and lead to land inundation. Effects of peat compaction on the natural evolution of deltas are however poorly understood, whereas this might be an important control on delta evolution at both local and regional scales.

The main objective of this paper is to review current knowledge concerning the peat compaction process and its effect on delta evolution in Holocene settings, and to identify gaps in this knowledge. An overview is given regarding: 1) the compaction process, 2) presumed and potential effects of peat compaction on delta evolution, 3) field methods to quantify peat compaction and 4) numerical models to calculate the amount and rate of peat compaction.

Peat compaction and formation influence channel belt elevation, channel belt geometry and channel belt configuration. Last-mentioned aspect mostly concerns the influence of peat compaction on avulsion, which is one of the most important processes controlling delta evolution. Interactions between peat compaction, peat formation and avulsion have seldom been studied and remain unclear, partly because factors such as peat type, organic matter content, sediment sequence composition and groundwater table fluctuation are so far not taken into account. Peat compaction and formation potentially influence avulsion as 1) a decrease in accommodation space created by peat compaction underneath a channel causes superelevation and/or an increase in lateral migration, 2) the high cohesiveness of peat banks inhibits lateral migration, which increases bed aggradation, decreases sediment transport capacity and hence increases crevassing frequencies, which possibly evolve into an avulsion, although the low regional gradient in peatlands will hinder this, and 3) peat compaction and oxidation in flood basins following groundwater table lowering leads to relief amplification of channel belts. At delta scale, variations in compaction rates might stimulate the occurrence of nodal avulsions.

To quantify effects of peat compaction on delta evolution, and to determine the relative importance of different factors involved, field research should be combined with numerical models describing peat compaction and formation. The model should be validated and calibrated with field data.

Contents

1. Introduction . . . 36
   1.1. The compaction process . . . 36
   1.2. Compaction due to biological processes . . . 37
   1.3. Compaction due to chemical processes . . . 37
   1.4. Compaction due to physical processes . . . 38
   1.5. Compaction potential of different soil types . . . 39
2. Effects of peat compaction and formation on delta evolution . . . 40
   2.1. Effects on surface topography . . . 40
   2.2. Geometry of channel and natural levee deposits . . . 40
   2.3. Avulsion . . . 42

* Corresponding author. Tel.: +31 302532779; fax: +31 302531145.
E-mail address: s.vanasselen@geo.uu.nl (S. van Asselen).

0012-8252/$ – see front matter © 2008 Elsevier B.V. All rights reserved.
doi:10.1016/j.earscirev.2008.11.001

3. Field methods to quantify peat compaction . . . 43
3.1. Dry bulk density . . . 43
3.2. Lithostratigraphy, basal peat and ^{14}C dating . . . 44
3.3. Measuring surface elevation change . . . 45
3.4. Deformation of logs . . . 45
4. Compaction models . . . 45
4.1. Empirical models . . . 45
4.2. Geotechnical models . . . 46
4.2.1. Models describing one-dimensional compression . . . 46
4.2.2. Three-dimensional models . . . 47
4.2.3. One-dimensional models describing primary and secondary compression . . . 47
4.3. Discussion peat compaction models . . . 48
4.3.1. Peat compaction in alluvial architecture models . . . 49
5. Conclusions . . . 49
Acknowledgements . . . 50
References . . . 50

1. Introduction

The evolution of deltas is largely controlled by 1) sediment supply and discharge, 2) substrate composition and topography, 3) base level fluctuations, 4) climate and 5) vertical land movements. The last-mentioned process may be due to tectonics, isostacy and compaction of unconsolidated sediments. Compaction is a process by which the porosity of a sediment is reduced, and involves micro-biological (e.g., organic matter decay), hydro-chemical (e.g., silica solution, cementation, clay dehydration) and physical processes (e.g., settlement, pore water expulsion), acting at different stages during the vertical accumulation within one system (e.g., Allen, 1999; Fig. 1). This paper focuses on physical processes causing compaction, occurring at shallow depths (0–10^1 m below surface) in Holocene fluvial–deltaic settings.

Especially in distal parts of modern deltas, which are often densely populated, peat is common. As peat has the highest compaction potential of all natural soils, compaction of peat potentially leads to substantial amounts of land subsidence. This may result in many societal implications including damage to construction works and relative sea-level rise causing e.g. coastal wetland loss and land inundation. In areas reclaimed for agriculture or habitation, land inundation often requires artificial lowering of the groundwater table. In such situations, compaction and oxidation of peat above the groundwater table leads to even more land subsidence and hence, ongoing lowering of the groundwater table is needed to prevent inundation. Groundwater extraction for economic purposes also increases subsidence rates (Abidin et al., 2001; Chen et al., 2003; Ericson et al., 2006; Rodolfo and Siringan, 2006; Teatini et al., 2006).

The effect of peat compaction on the natural evolution of Holocene fluvial–deltaic environments and hence on the alluvial architecture is poorly understood however. Alluvial architecture is defined as the geometry, proportion and spatial distribution of different types of fluvial deposits in an alluvial succession (Allen, 1978; Leeder, 1978). A detailed understanding of the alluvial architecture is vital for e.g. exploration of natural resources (oil, gas, water, metals) and for construction works, which need a solid incompressible substrate. A principal factor controlling alluvial architecture is avulsion (Bridge and Leeder, 1979; Smith et al., 1989; Stouthamer, 2001), which is a natural process by which a channel belt is abandoned in favor of a new course. Although Gouw (2007) recognized compaction as a factor influencing alluvial architecture in the Mississippi delta and the Rhine–Meuse delta, our knowledge about its role is still limited.

The main objective of this paper therefore is to review current knowledge concerning the peat compaction process and its effect on delta evolution at Holocene timescales, and to identify gaps in this knowledge. Therewith, this paper serves as a starting point for future research regarding effects of peat compaction in Holocene fluvial–deltaic settings.

1.1. The compaction process

Compaction is one of the most important processes leading to vertical land subsidence, besides processes as isostacy and tectonics (e.g., Kooi and De Vries, 1998; Shennan and Horton, 2002). Also, it is the first step in lithification, the process in which unconsolidated sediments are converted into sedimentary rocks. After the sediments have been compacted, cementation by dissolved minerals transforms loose sediment into rock. In some environments cementation may occur prior or simultaneously with compaction. In such situations, cementation may influence the compaction potential as pore space is filled with cement, which finally leads to less subsidence due to (mechanical) compaction (Clari and Martire, 1996). In peat however, this will be uncommon.

Compaction does not always lead to *subsidence*. This can be illustrated by considering a situation in which a uniform peat layer overlies an incompressible subsurface (Fig. 2). In this scenario, it is assumed that peat growth can keep up with the rate of groundwater table rise. Close to the incompressible surface the pressure exerted by the thick overlying sediment sequence (expressed in vertical effective stress, see Section 1.4) is greatest, so the amount of compaction will be high, but the amount of subsidence is close to zero as the underlying substrate is incompressible (assuming there are no other causes of subsidence). For a uniform sediment sequence, the maximum amount of lowering therefore occurs in the middle of the sequence. At this

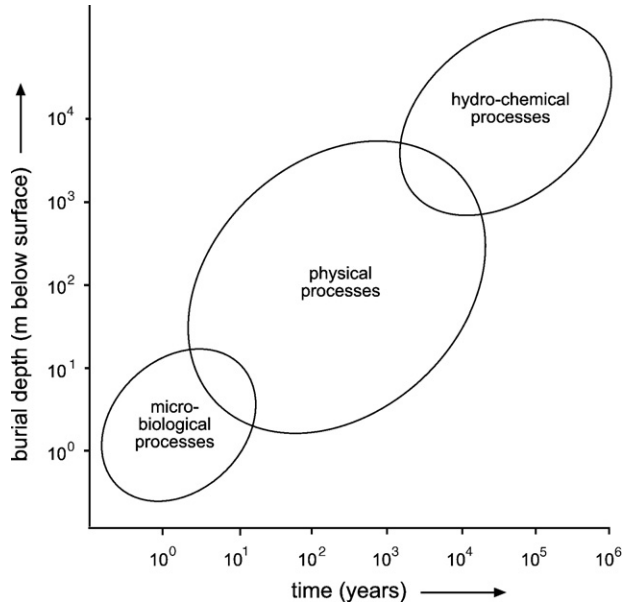

Fig. 1. Dominant processes leading to compaction at different burial depths and timescales.

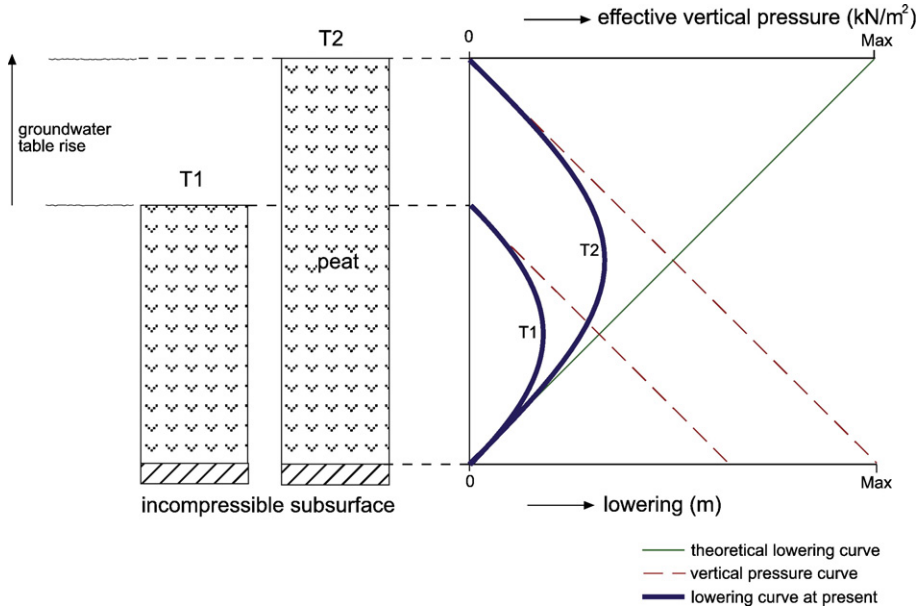

Fig. 2. Vertical lowering within a sequence due to compaction. For a uniform sediment sequence maximum lowering occurs in the middle of the sequence. It is assumed that peat accumulation keeps up with groundwater level rise.

point, an optimum exists for the amount of compressible sediment below this point and the load above this point. A similar lowering profile is described by compaction models of e.g., Pizzuto and Schwendt (1997), Paul and Barras (1998) and Massey et al. (2006), and is shown by field data from the Rhine–Meuse delta (unpublished).

Although physical processes are considered to be most important regarding compaction at Holocene timescales, some biological and chemical processes can be important as well, as outlined in the following sections.

1.2. Compaction due to biological processes

Considering compaction of peat, a significant amount of the volume reduction occurs during the peat formation phase, mainly due to *microbiological processes*. In principal, peat formation is initiated in wet environments with low mineral input where production of organic matter exceeds decay. The balance between production and decay of organic matter determines the peat accumulation rate. This balance is primarily controlled by the decay rate (largely a result of microbial decomposition), which is influenced by temperature, water content, oxygen supply, microbial and soil animal population and plant material (Charman, 2002). As these factors are highly variable (spatially and temporally), the production and decay rates, and therewith the rate of volume reduction due to biological processes, are also highly variable (for an overview of peat accumulation, production and decay rates is referred to Charman, 2002). A clear distinction can be made though between rates in the acrotelm (top soil layer which is at least seasonally aerated) and the catotelm (permanently waterlogged): productivity and decay will be highest in the acrotelm, as in this zone conditions for plant growth and soil fauna are most favorable.

Latter et al. (1998) demonstrated, based on litter bag experiments on a peat bog in upland Britain, that rate of biomass loss is highest during the first couple of years (Fig. 3). The rate depends on the type of litter, although after 23 year the percentage of the initial weight remaining for all litter types was similar (about 40–50%).

1.3. Compaction due to chemical processes

Oxidation of organic matter is considered to be an important chemical process leading to volume reduction of a soil layer, and hence to land subsidence (e.g., Gambolati et al., 2006). The amount of biomass loss due to oxidation will be highest in the acrotelm. The depth of this zone may be enlarged by natural or artificial groundwater table lowering. For example, in the Netherlands, flood basins were artificially drained for agriculture ('polders') since approximately 1000 AD, while the main rivers consecutively were embanked (Fig. 4). This has induced significant land subsidence in the flood basins due to oxidation and compaction, which led to additional groundwater table lowering and hence further land subsidence, causing huge problems in this densely populated area.

Schothorst (1977) studied subsidence of peat soils in the western Netherlands. At different experimental fields, groundwater tables were maintained at different levels, ranging from 0.25 to 1.00 m below the surface. After 6 years surfaces had subsided up to 10 cm (16.7 mm/yr). The highest amount of subsidence occurred at sites where the groundwater table was relatively low. Based on periodic altitude measurements of metal disks placed at regular intervals in vertical peat sections, Schothorst (1977) concluded that on average 65% of the total subsidence was due to compaction following a decrease in hydrostatic pressure and oxidation of organic matter in the layer above groundwater

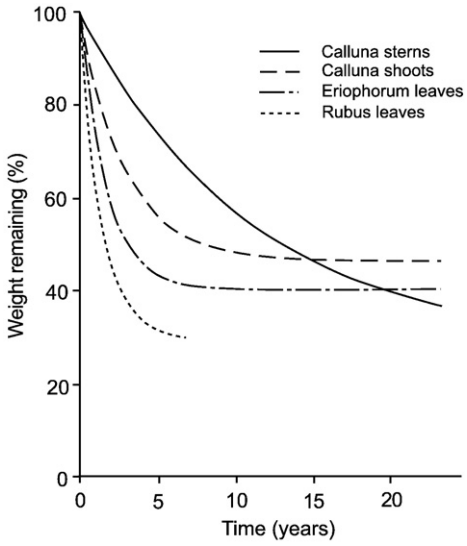

Fig. 3. Percentage of litter weight remaining with time (from Latter et al., 1998).

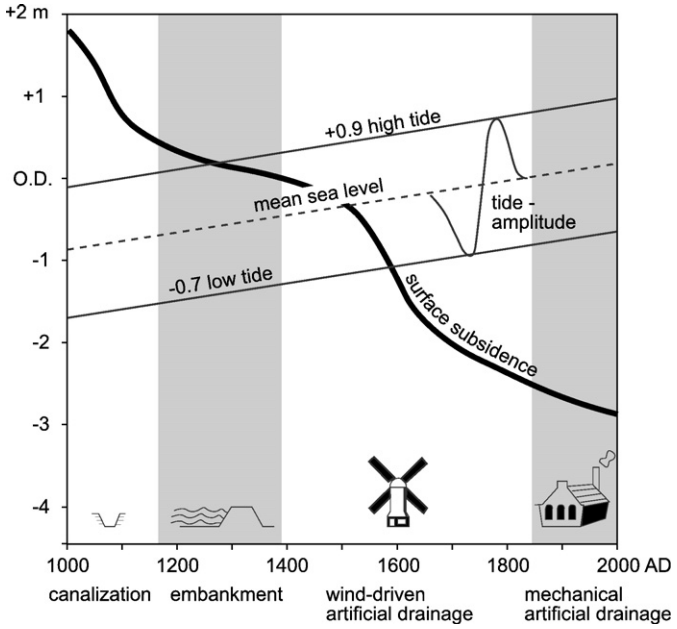

Fig. 4. Subsidence of a peat surface in The Netherlands as a result of canalization, embankments and artificial drainage since 1000 AD (after Berendsen, 2000).

table, and about 35% was attributed to compaction of the layer below the groundwater table.

Another study in a Dutch polder (Beuving and van den Akker, 1996) demonstrated that a groundwater table kept for 25 years at 0.3–0.35 m below the surface leads to subsidence of 0.167 m (6.7 mm/year). A groundwater table kept at 0.70 m below the surface for the same time period led to 0.396 m subsidence (15.8 mm/year).

1.4. Compaction due to physical processes

Compaction caused by physical processes can be explained by changes in *effective stress* (σ'), which is defined as the difference between the total stress (σ) and the pore water pressure (u) (Eq. (1); Fig. 5; Terzaghi, 1943).

$$\sigma' = \sigma - u, \tag{1}$$

During compaction, soil particles are packed more closely together which results in a decreased porosity and increased bulk density. Eq. (1) implies that an increase in total stress and/or a decrease in pore pressure causes an increase in effective stress and hence induces compaction. In natural situations, the total stress imposed on a sediment layer is increased due to loading by active deposition. Pressure induced by heavy machinery and construction works also increase the total stress.

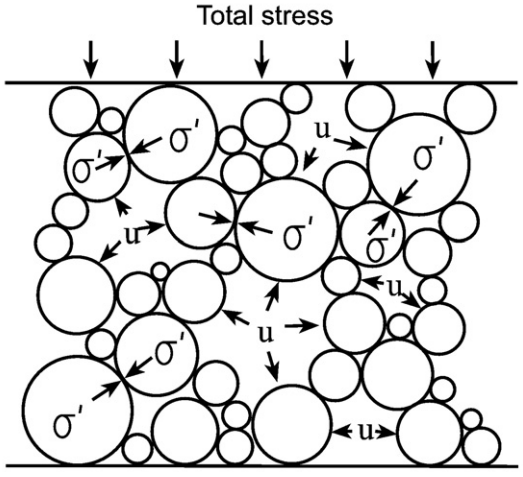

Fig. 5. Schematic representation of the effective stress (σ'=total stress − pore water pressure) in a soil. The total stress (σ) is the weight of the overlying soil and external load per square meter above a certain level in the soil.

A decrease of the pore water pressure is in natural situations caused by groundwater table lowering e.g., due to sea level lowering or evaporation. A human-induced decrease of the porewater pressure can be the result of artificial groundwater table lowering for land reclamation and withdrawal of drinking water, oil and gas in older deltaic sequences (e.g., Kooi and De Vries, 1998).

The physical compaction process can be subdivided into compression and consolidation (e.g., Paul and Barras, 1998; GeoDelft, 2003). *Compression* is the instantaneous decrease in soil volume due to a stress-dependent rearrangement of the internal sedimentary structure. *Consolidation* is the volume reduction of a soil due to the time-dependent expulsion of overpressured pore water, occurring while the sediment structure approaches a new equilibrium at an extra applied load. In fine-grained sediments with low permeability, such as clay and peat, dissipation of excess pore pressure might take considerable time. The time-duration of the consolidation process is called the *hydrodynamic period* (or primary compression). After this period the soil continues to settle, which is called *secondary compression* (sometimes indicated as *creep*). Causes of secondary compression are not completely understood (GeoDelft, 2003). Possible explanations are (1) long-term deformation of the thin water layer that coat clay particles, due to high pressures on the soil mass, or (2) expulsion of excess pore water pressure from extremely small voids, which was not expelled during the hydrodynamic period. The start of secondary compression is also a topic of debate; some researchers believe it starts after the hydrodynamic period has ended (e.g., Terzaghi, 1943), while others think it occurs directly after loading and continues for a very long time (e.g., Buisman 1940; Bjerrum, 1967; for a detailed discussion see Den Haan, 1994).

In geotechnical studies, compressibility characteristics of sediments are usually determined with *oedometer* tests (Fig. 6). One of the most important assumptions made in oedometer tests is that there is no lateral strain (only vertical compaction) and that the sediment is considered to be homogeneous.

Soil behaves differently under conditions of loading, unloading and subsequent reloading, which is visualized in the stress–strain figure resulting from an oedometer test (Fig. 7). The maximum effective stress a sample has experienced in the soil is called the *preconsolidation stress* (σ'_c). A sample taken from the soil will first experience a load release, following the relaxation curve b–c in Fig. 7 (gradient C_1). During reloading, settlement will follow the same curve in the opposite direction (recompression curve c–d) until the preconsolidation stress is reached. Soils in conditions represented by these curves are considered to be overconsolidated, which means that the soil has

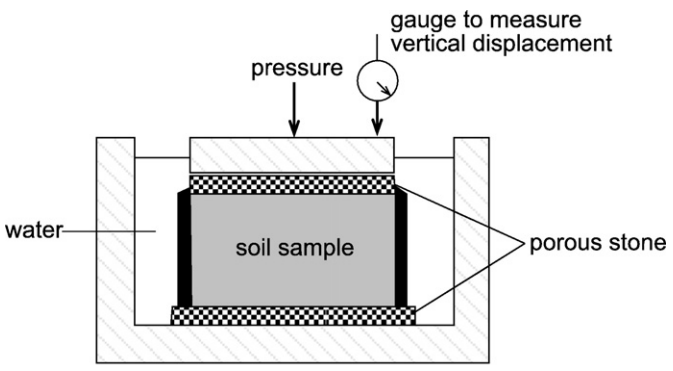

Fig. 6. Schematic representation of an oedometer, in which one-dimensional compression or swell can be measured, resulting from increasingly applied vertical pressure.

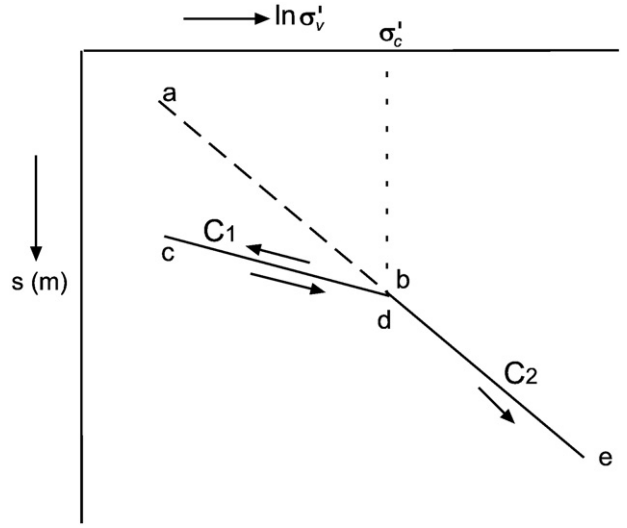

Fig. 7. Schematized stress–strain diagram (s = vertical deformation, σ'_v = vertical effective stress, σ'_c = preconsolidation stress, $C_{1/2}$ = compression coefficients, after GeoDelft, 2003). Soils subjected to load release or to reloading follow curve b–c–d, soils subjected to higher stresses than they have experienced before follow curve a–b–e.

been subject to an effective pressure greater than the pressure of the present overburden. Further loading of a sample beyond the preconsolidation stress results in a higher compressibility (steeper slope of the stress–strain line; C_2); curve a–b–e is called the *virgin compression line*. Soils in such conditions are indicated as normally consolidated.

During loading overpressured pore water is expelled and mineral grains are rearranged, fractured and distorted by compression. During unloading the soil takes up water again, but the fractured and rearranged soil matrix will not recover to its initial state. This explains why the volume change is less for un- and reloading (less steep gradient) compared to loading of normally consolidated soils.

1.5. Compaction potential of different soil types

A soil is composed of organic matter, minerals and pore space, which is filled with air (gasses) and/or water. The compaction potential of a specific soil depends on the following factors:

(1) Initial porosity. Soils with a high initial porosity have a higher compaction potential than soils with a low initial porosity.
(2) Water content (percentage of pores that are filled with water). Water acts to decrease friction between soil particles, which makes moist soil easier to compact compared to dry soil. However, if a soil is too wet, water carries part of the load of the soil, which will lead to a lower compaction potential.
(3) Soil texture (percentage of sand, silt and clay). Soils with particles of about the same size compact less than soils consisting of particles with variable size. In the last case, small particles can fill pores between larger particles making the soil denser.
(4) Organic matter content. Organic matter is often used to improve the fertility of a clastic (agricultural) soil. This also makes the soil more resistant against compaction as soil structure is improved. However, natural organic soils such as (clayey) peat have a high compaction potential due to its low mineral content and high initial porosity. Most likely, the clastic content and type of peat forming plant species (e.g., wood, herbal plants or mosses) will influence the compaction potential.

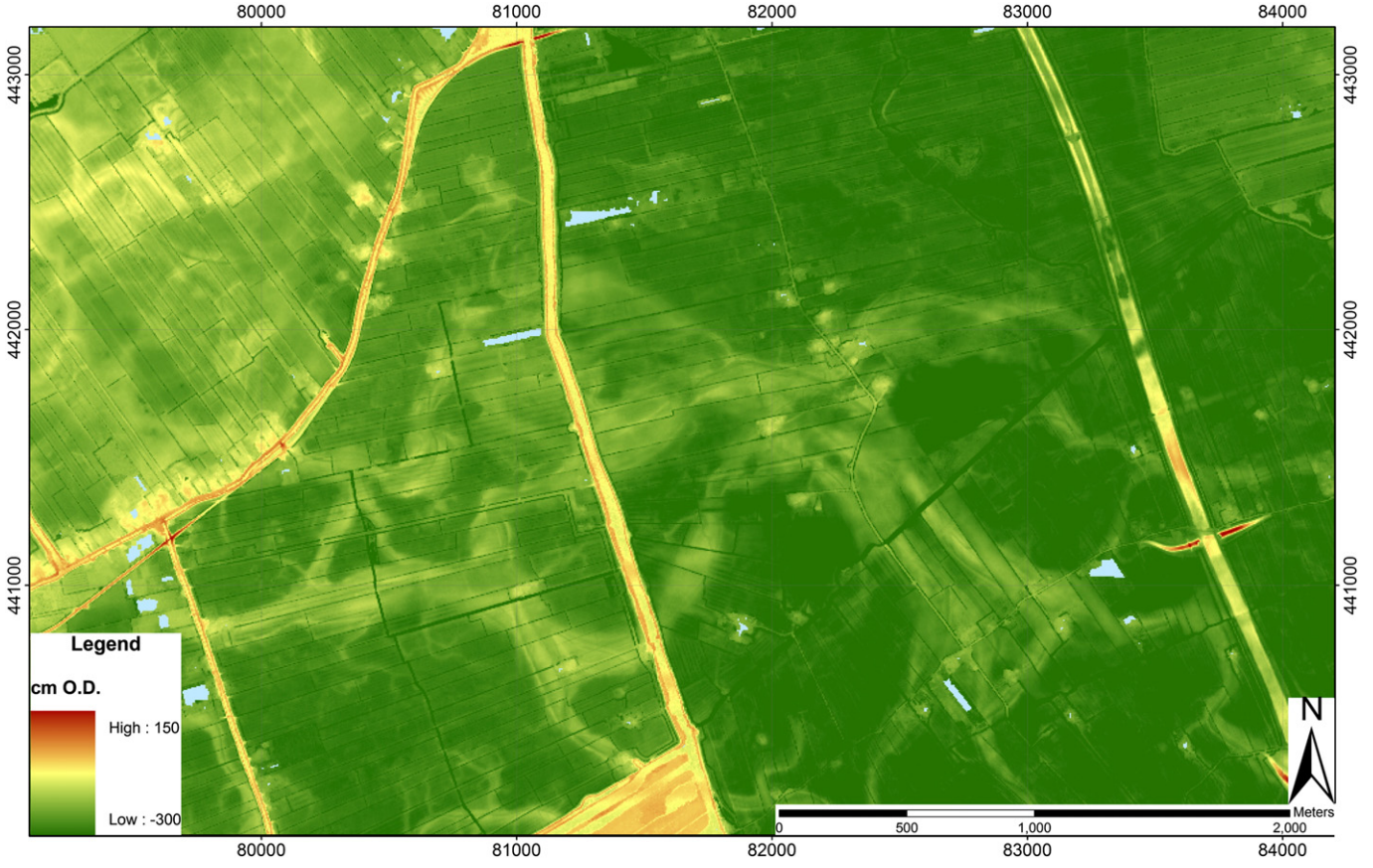

Fig. 8. Digital Elevation Model (DEM; 5 m resolution, Dutch coordinate system). Levees appear as ridges in the landscape after compaction of peat and clay in the floodbasins (near Rotterdam, western Netherlands) (Rijkswaterstaat-AGI, 2005). See also Berendsen and Vollenberg (2007).

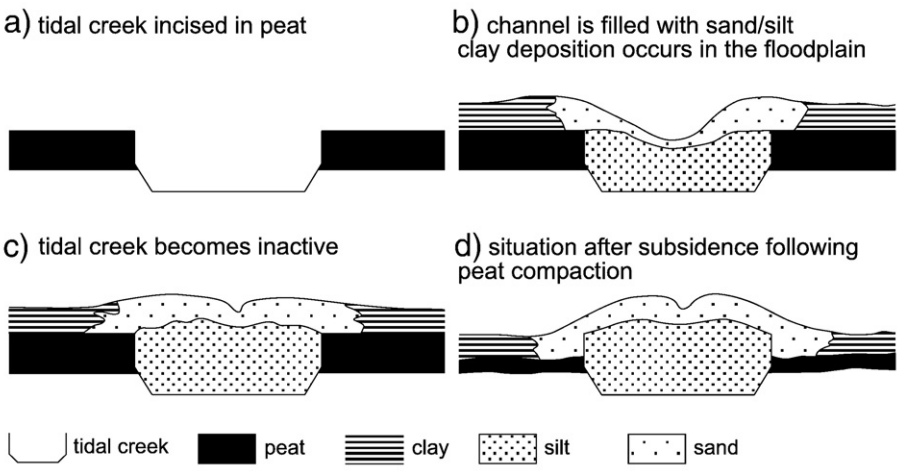

Fig. 9. Schematic representation of relief inversion of tidal creeks (after Berendsen, 2005).

In general, sands and gravels are nearly incompressible, clays compact to a moderate degree and peat is highly compressible (Allen, 1999). Land subsidence due to compaction is largely controlled by the spatial distribution of deposits with different soil textures, overlying load, compaction response time (hydrodynamic delay) of sediment layers (Kooi and De Vries, 1998) and groundwater table fluctuations.

2. Effects of peat compaction and formation on delta evolution

2.1. Effects on surface topography

A well-known effect of differential compaction of lithologically diverse sediment sequences is distortion of the original stratigraphy, and of the surface topography (e.g., Allen, 1999, 2000; Amorosi and Milli, 2001). In a situation of groundwater table lowering, compaction and oxidation of peat may lead to:

1) Amplification of the surface topography. In general, channel and natural levee deposits consist of sand and silt, while further away from the channel (in the flood basin) peat and clay dominate the sediment sequence. As peat and clay are more compressible, land subsidence due to compaction and oxidation of peat is greater in the flood basins. Consequently, the elevation of the channel belts is amplified (Fig. 8).
2) Relief inversion. This occurs for example in intertidal areas. Initially, tidal creeks incise in peat and clay deposits and form low-lying channels. After abandonment, the sand-filled channels appear as ridges in the landscape as sand is less susceptible to compaction and oxidation than peat and clay deposits in the surrounding flood basin (Fig. 9; Vos and Van Heeringen, 1997; Berendsen, 2005; Spijker, 2005).

2.2. Geometry of channel and natural levee deposits

Subsidence due to compaction of peat creates accommodation space for (e.g., fluvial) deposition, thereby increasing sedimentation rates, as was demonstrated by a field study of Haslett et al. (1998). Results of a modeling study of Allen (1999) supported this idea. Peat

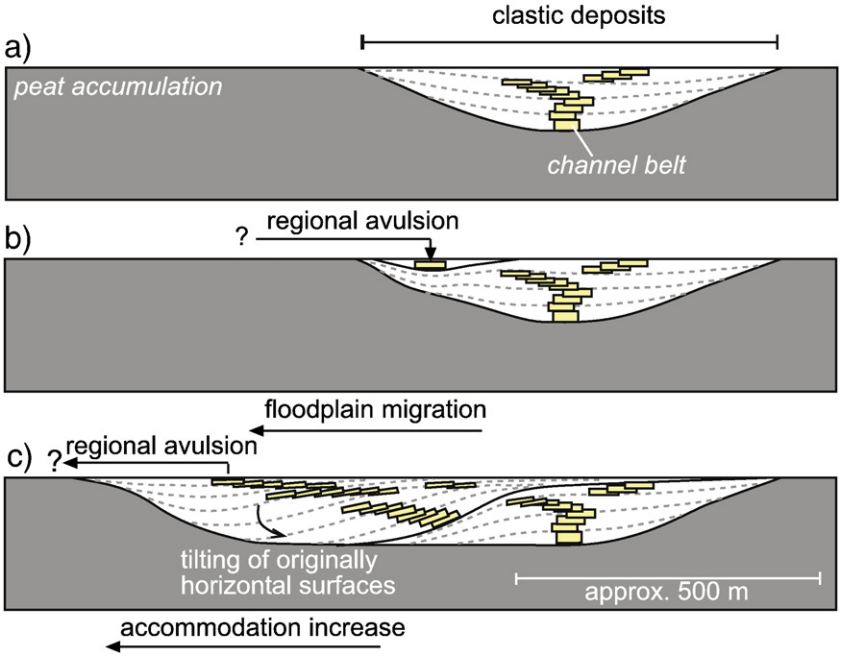

Fig. 10. Schematic cross-section representing the evolution of clastic deposits on top of compacting peat according to Rajchl and Uličný (2005). a) Local avulsions within a clastic deposit associated with one river system, b) regional avulsion leads to the beginning of evolution of another avulsion sequence and c) differential compaction across a floodplain causes gradient advantages leading to regional avulsions.

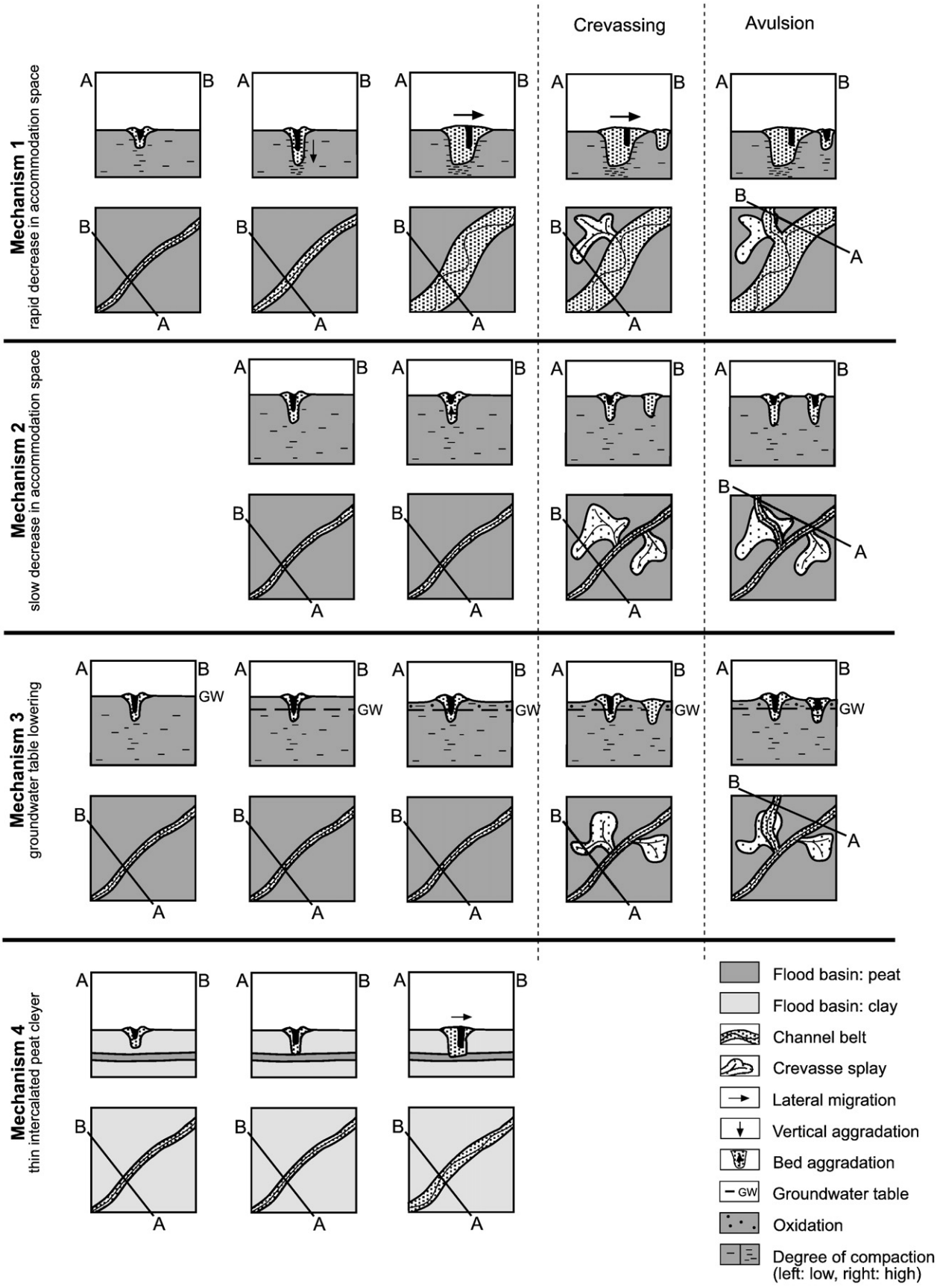

Fig. 11. Schematic representation of possible influences of peat compaction and formation on river behaviour. Crevassing, and hence possibly avulsion, may be initiated by an increased tendency for lateral migration due to a decrease in the rate of accommodation space created by peat compaction (mechanism 1), by bed aggradation and the associated lower sediment transport capacity, caused by the high cohesive peat banks (mechanism 2) and by superelevation of the channel belt due to peat compaction and oxidation in flood basins following groundwater table lowering (mechanism 3). Mechanism 4 shows that an intercalated peat layer may lead to channel belts with a high width/depth ratio.

underlying a river channel will be compacted (if not eroded) due to the load of channel deposits. Provided that the sediment load of the river is sufficiently high, accommodation space created by peat compaction will be filled by increased within channel sedimentation. This leads to vertical aggrading river channels (e.g., Michaelsen et al., 2000; Rajchl and Uličný, 2005) with a low width/depth ratio. Similarly, peat compaction underneath natural levees can result in thick natural levees.

The geometry of river channels is also affected by the high cohesiveness of a peat substrate, besides other factors as stream power and aggradation rate (Törnqvist, 1993; Makaske, 1998, 2001; Gouw and Berendsen, 2007). A cohesive subsoil (like peat), low stream power and a high aggradation rate (e.g., due to sea level rise) are favorable conditions for the development of channels with a low width/depth ratio. According to Gouw and Berendsen (2007) bank stability caused by river dissection of a peat substrate was the dominating factor leading to relatively deep and narrow channels in the Holocene Rhine–Meuse delta. Low sediment supply may be an additional factor leading to laterally stable channels. Contrary, if an incising channel encounters an intercalated peat layer it will first erode to the depth of the peat layer, which then due to its resistance prevents further vertical incision resulting in channels with a high width/depth ratio (Smith and Pérez-Arlucea, 2004; Fig. 11 mechanism 4).

2.3. Avulsion

Avulsion is regarded as one of the most important processes influencing delta evolution, and hence, alluvial architecture. The occurrence of avulsion is influenced by climate, tectonics, base level change, discharge variations, substrate composition, human influence and local factors such as ice and log jams (Stouthamer and Berendsen, 2000). The influence of peat compaction and formation on avulsion has seldom been investigated. The few existing conceptual sedimentary models concerning this topic are based on exposures of old sediment sequences presently comprising coal layers (Michaelsen et al., 2000; Rajchl and Uličný, 2005). These sequences show the end-product of numerous processes that have acted over a long time period. Partly based on these studies, ignoring the difference in time scale, potential influences of peat compaction on avulsion in Holocene settings are derived:

1) When a river invades a peatland, accommodation space is created by peat compaction underneath the channel, which initially leads to vertical aggradation. Through time, the rate of accommodation space created by peat compaction, due to loading by channel belt deposits, decreases. This results in a greater tendency for lateral migration, a higher sinuosity and a decrease in downstream channel slope (Rajchl and Uličný, 2005). As a result, the river becomes more prone to avulsion (Fig. 11: mechanism 1). The resulting alluvial architecture at floodplain scale is shown in Fig. 10.
2) The combination of the high cohesiveness of river banks consisting of peat, low stream power and low regional gradients in peatlands inhibits lateral migration of rivers (Fig. 11: mechanism 2). Instead, bed aggradation is favored, which reduces channel flow and sediment transport capacity (Stouthamer and Berendsen, 2007). This results in frequent crevassing of the main channel, which is an important mechanism initiating avulsion (Smith et al., 1989). However, it should be noted that due to the low regional gradients common in peatlands, crevasses often fail to evolve into an avulsion. The occurrence of either mechanism 2 or mechanism 1 depends on the balance between the rate of accommodation space created by peat compaction (v_{as}) and the sediment load of the river. A relatively low v_{as} and high sediment load will favor mechanism 2. The v_{as} is influenced by the weight of overlying deposits and peat type, ignoring other causes of creating accommodation space.
3) In a situation of groundwater table lowering, flood basin subsidence due to compaction and oxidation of peat above the groundwater table induces superelevation of the channel belt (Fig. 11: mechanism 3; see also Section 2.1). Superelevation of a channel or channel belt above the floodplain, and the associated increase in the cross-valley slope (s_{cv})/down-channel slope (s_{dc}) ratio, increases the risk of avulsion (e.g., Heller and Paola, 1996; Stouthamer and Berendsen, 2007). The s_{cv}/s_{dc} ratio is by some authors regarded as one of the most important controls on avulsion (e.g., Törnqvist and Bridge, 2002). Field data from the Mississippi River floodplain showed however that gradient advantages are not fully responsible for the occurrence of avulsion (Aslan et al., 2005; Stouthamer and Berendsen, 2007).
4) At a larger temporal and spatial scale, variations in compaction rate across the floodplain influence regional topography, which potentially lead to a shift of the river system to a formerly uninvaded part of the floodplain. Different compaction rates might occur due to for example variations in thickness and composition of the Holocene sediment sequence and peat type. Furthermore, the low regional gradient of peatlands causes a sudden drop in channel belt gradient at the point where the river enters the peatland, resulting in deposition of relatively coarse clastics at

Table 1
Overview of field methods used to quantify peat compaction

Method		Study site	Measured amount of compaction	Over burden	Subsidence rate (due to compaction)	Accuracy	Spatial scale	Time scale	Source
Relation bulk density with LOI/texture		Intertidal zone coast Singapore	0–67%; (calculated for 10 cm intervals)	Up to 9 m; variable composition	–	Intermediate	Small	Large	Bird et al. (2004)
Stratigraphic cross-sections and ^{14}C dating of basal peat		SW Britain, Connecticut (USA), Mississippi Delta (USA)	13–47%	Up to 3.16 m; clay	5 mm/yr	High	Intermediate	Large	Haslett et al. (1998), Bloom (1964), Törnqvist et al. (2008)
Surface elevation measurements	Surface Elevation Table	Salt marshes Louisiana, Florida and North Carolina (USA)	–	–	2.25–24.5 mm/yr (mean rates; upper 5 m)	High	Small	Small	Cahoon et al. (1995, 2000) / Rogers and Saintilan (2006)
	Levelling/GPS survey	Jakarta, Indonesia	–	–	80–267 mm/yr (mean rates)[a]	Low	Intermediate	Small	Abidin et al. (2001)
	High resolution DEMs	Coachella Valley, California (USA)			Up to 90 mm/yr[a]	High	Large	Small	Galloway et al. (1998)
Deformation of logs		Boston (Kaye and Barghoon), Florida (Stout and Spackman)	20–45%	Up to few meters	–	Low	Small	Large	Kaye and Barghoon (1964) / Stout and Spackman (1989)

[a] High rates due to artificial groundwater extraction.

these sites. These conditions favor the occurrence of regional (nodal) avulsions at the edges of peatlands (e.g., Morozova and Smith, 2000; Rajchl and Uličný, 2005).

Conceptual models regarding the influence of peat compaction on avulsion do not address the influence of factors such as peat type (plant composition), organic matter content of the peat, sediment sequence composition, sediment load and river discharge, and rate of fluvial sedimentation on the amount and rate of compaction in different fluvial settings. Plant composition influences peat structure, which might affect the compaction potential, and the resistance of a peat substrate to fluvial erosion. Organic material is more compressible than clastic material, so a high organic matter content probably leads to a higher compaction potential. Loading by fluvial deposits will lead to compaction of underlying peat, but the amount of compaction will depend on the thickness and composition of the overlying clastic sediment layer, and of the depositional environment.

Detailed field studies in modern floodplain areas are needed to determine and quantify the relative importance of such factors on peat compaction and hence on the evolution of fluvial–deltaic environments.

3. Field methods to quantify peat compaction

3.1. Dry bulk density

The dry bulk density of unconsolidated sediments generally increases due to compaction following external loading (e.g., Craig, 1987; Kruse, 1998) or groundwater fluctuations (Kool et al., 2006; Whittington and Price, 2006). Bird et al. (2004) found relations between the bulk density, texture and organic matter content of uncompacted peat samples and used these to calculate the uncompacted bulk density of compacted Holocene sediments (Table 1). In this way, the amount of subsidence due to compaction could be calculated. Both the compacted and uncompacted sediment samples were taken from mangrove regions (intertidal zone; compaction above sea-level may occur during low tides) along the coast of Singapore. The percentage of compaction for three mangrove sediment sequences (in which a peat layer underlies a clastic sediment layer of up to ~9 m, partly due to recent landfill material) calculated over 10 cm intervals ranged from 0 to 67%. Based on their results they concluded that organic rich and/or fine grained sediments were more susceptible to compaction than inorganic sands. However, a closer examination of their results shows that peaks in the percentage of compaction especially seem to correlate with peaks in the fraction <63 μm and less with the organic matter content (Fig. 12).

The amount of compaction calculated over 10 cm intervals sometimes drops to zero, though the LOI (loss on ignition) of the >63 μm fraction is >80%. This seems very unlikely as high organic peat is highly compressible. Furthermore, their sampling technique probably caused some disturbance of the sediments, which might have influenced their results; a PVC tube of 3.8 cm in diameter was pushed into the sediment surface. Peat often has a loose structure, and peat characteristics are highly variable, for example due to the inclusion of wood fragments. Field studies on physical properties of soils have shown that dry bulk densities of different peat types from different areas vary in the range of 0.01 to 0.4 g cm^{-3} (e.g., Brandyk et al., 2002; Price et al., 2005; Whittington and Price, 2006). Moreover, Price et al. (2005) investigated relationships between the compressibility of peat, bulk density, fibre content and the state of peat decomposition, expressed by the 'Von Post number'. The only significant correlation they found was between virgin compressibility and bulk density at one location (in one core).

To take into account the heterogeneity of peat characteristics, sufficiently large samples should be taken when determining peat characteristics such as dry bulk density and organic matter content. Furthermore, it is vital not to disturb the peat structure during sampling. Special sampling devices should be used, such as the block sampler of Lefebvre et al. (1984). This device takes cylindrical shaped block samples by using sharp cutting blades, which rotate while moving down to carefully cut the fibres in the peat. The Wardenaar corer is another device that may be used for taking relatively undisturbed peat samples (Wardenaar, 1987). This corer consists of two rectangular boxes with sharp cutting edges at the lower ends. The two halves can be pushed into the soil alternatingly to take relatively undisturbed peat cores of 10×10×100 cm. A modified Wardenaar corer with larger dimensions (15×15×100 cm) and a serrated cutting edge was developed by Givelet et al. (2004). Buttler et al. (1998) developed a peat sampler consisting of two concentric tubes, whereby the outer one is used as a cutter and the inner one as a collector. This sampler extracts cores of 13.3 cm in diameter and up to 70 cm long.

Provided that a suitable peat sampling device is used, it is suggested here that relations between the dry bulk density of compacted and uncompacted peat could be used to estimate the

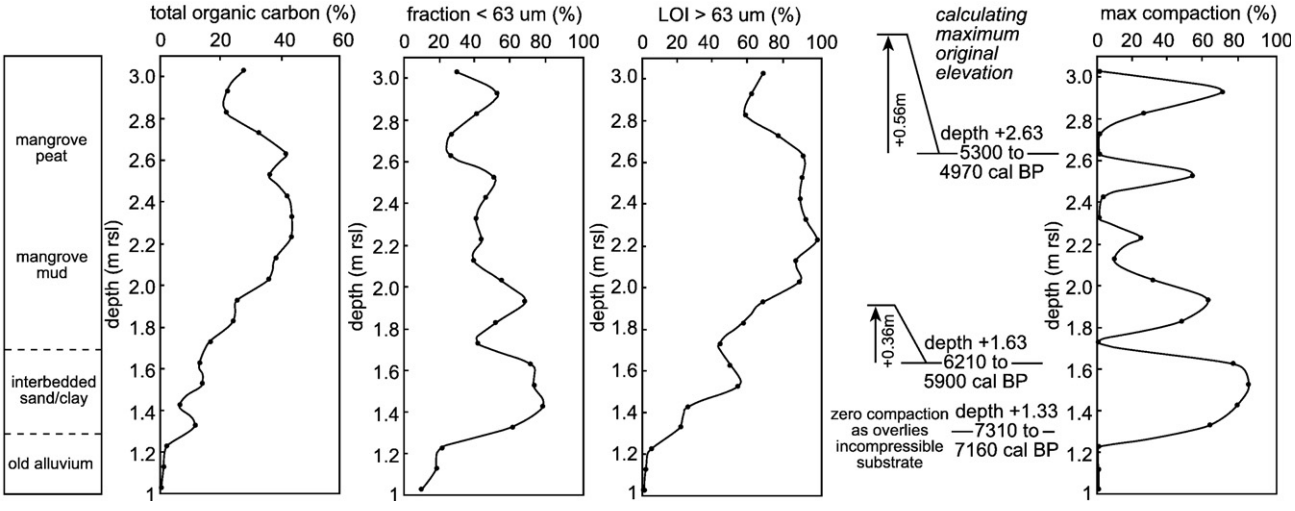

Fig. 12. Total organic carbon (%), fraction<63 μm (%), LOI>63 μm (%) and amount of compaction (%) plotted against depth for a core taken in a mangrove environment near Singapore (from Bird et al., 2004).

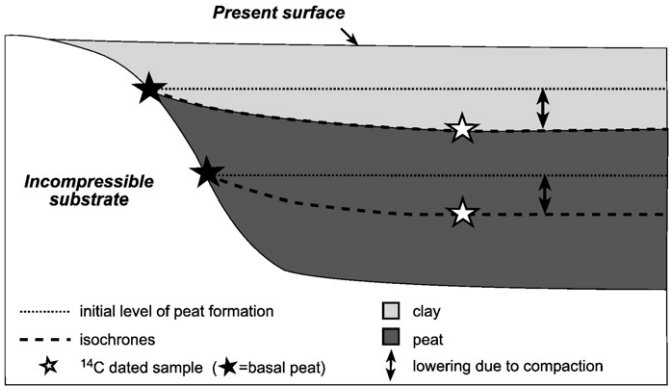

Fig. 13. Schematic representation of using stratigraphic cross-sections and ^{14}C dating of (basal) peat to estimate the amount of compaction.

decompaction height of compacted Holocene peat layers. Note that only bulk density values of peat of the same type can be compared.

3.2. Lithostratigraphy, basal peat and ^{14}C dating

Basal peat is formed directly on an incompressible substrate, and therefore, does not subside due to compaction. By dating basal peat and the peat profile in flood basins, which is susceptible to subsidence due to compaction, isochrones can be constructed (Fig. 13). The amount of subsidence due to compaction can now be calculated by assuming the initial level of peat formation is at the same altitude as the isochronous dated basal peat.

Haslett et al. (1998) used this method to estimate the amount of compaction at Somerset Levels, Britain (Fig. 14, Table 1). Three ^{14}C dated peat samples confirmed the top of the peat layer was isochronous. The minimum altitude of the original peat surface was estimated based on its maximum present altitude (distance 40 m in Fig. 14), where the peat is regarded as basal peat. The maximum difference between this altitude and the present minimum altitude of the top of the peat layer (distance 120 m in Fig. 14) indicated maximum compaction of 2.22 m (of a peat layer with an assumed original thickness of 4 m).

Bloom (1964; Table 1) used the same method in a tidal marsh in Connecticut, USA and found that in 7000 years the peat layer had compacted 13 to 44% of its original thickness.

Based on ^{14}C dating and an assumed initial level of peat formation, that was related to past mean sea level, Törnqvist et al. (2008; Table 1) calculated compaction rates of up to 5 mm/year on millennium-scale. On shorter timescales (10^2–10^3 years) they estimated rates of 10 mm/year. A linear relationship between compaction rate and overburden thickness was found.

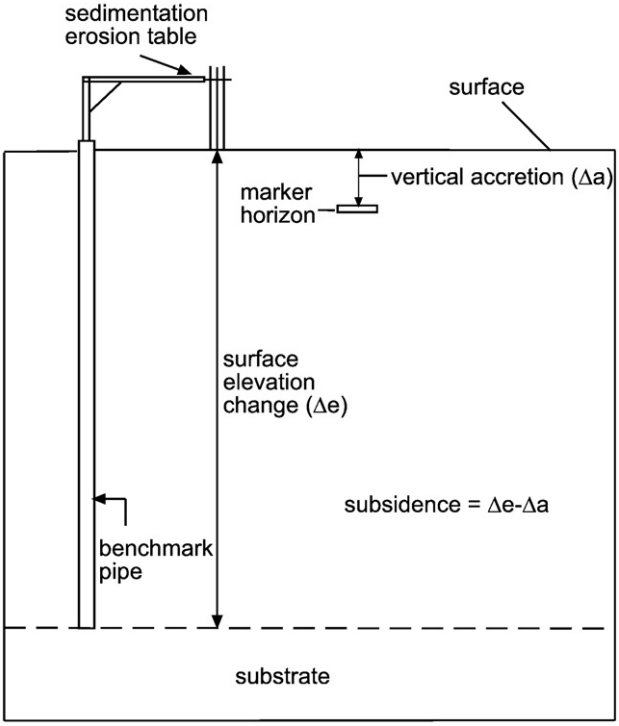

Fig. 15. Schematic representation of a Sedimentation Erosion Table (SET) and marker horizons. Shallow subsidence is calculated as vertical accretion minus elevation change. Adapted after Cahoon et al. (2000).

The method described in this section can also be used to investigate relations between the amount of compaction and fluvial deposition patterns, for example by constructing a cross-section from a channel belt towards the flood basin. To determine changes in boundary conditions through time, a detailed understanding of the paleogeographical development of the investigated area is needed, which requires detailed logging of many cores. The altitude of ^{14}C dates and surface topography should be measured accurately, which requires the use of leveling or differential (d)GPS for measuring surface elevation.

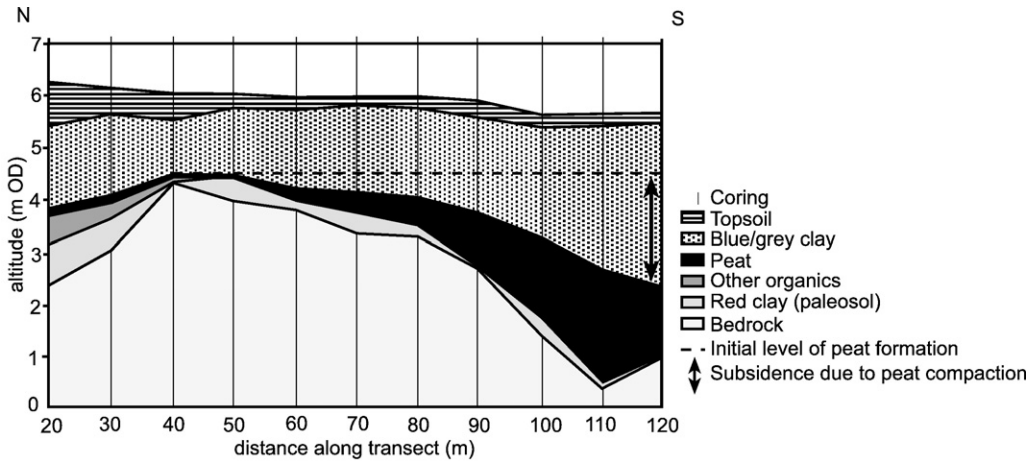

Fig. 14. Using a stratigraphic cross-section to calculate the amount of peat compaction. The former level of peat formation is estimated based on its maximum present altitude, at a side where it directly overlies incompressible bedrock. After Haslett et al. (1998).

3.3. Measuring surface elevation change

Surface elevation changes are measured by e.g., conventional leveling, (d)GPS surveys, high resolution Digital Elevation Models (DEMs) and Surface Elevation Tables (SET, see Boumans and Day, 1993; Fig. 15).

Last mentioned technique measures elevation changes from a fixed level above the surface. Vertical accretion is measured as the rate of sedimentation above marker horizons. The difference between accretion and elevation change is used to calculate the amount of shallow subsidence. The rate of compaction of newly deposited sediments can be determined by installing a second set of marker horizons after the start of measurements (Cahoon et al., 2000).

Using this technique, Cahoon et al. (1995, 2000; Table 1) measured vertical accretion and surface elevation change in salt marshes in Louisiana, Florida and North Carolina, USA, using feldspar marker horizons, which are easily distinguishable from the surrounding sediments. The objective of their study was to calculate the amount and rate of subsidence of the upper 5 m of soil. After two years, they had measured total vertical accretion by sediment deposition and plant production ranging from 7.7 to 51.9 mm (3.85 to 25.95 mm/yr) and total subsidence due to compaction of 4.5 up to 49.0 mm (2.25 to 24.5 mm/yr). At each site, surface elevation change was significantly lower than vertical accretion, due to compaction. This was also found by Rogers and Saintilan (2006; Table 1), who applied the same method at ten different sites in salt-marshes and mangroves in southeast Australia. After three years of measuring, compaction rates varied considerably between the different sites, with values of up to 11.62 mm/yr. Differences in compaction rates between sites were attributed to different bulk densities, mineral and organic matter contents, rainfall and plant production rate.

Abidin et al. (2001; Table 1) used leveling and GPS surveys to estimate land subsidence rates in Jakarta, Indonesia. Based on leveling surveys, up to 800 and 1600 mm subsidence for the periods 1982–1991 (mean rate of 89 mm/yr) and 1991–1997 (mean rate of 267 mm/yr) respectively was measured. Based on a GPS survey 200 mm of subsidence for the period of 1997–1999 (mean rate of 100 mm/yr) was calculated. Thus, on average, the highest rates of subsidence occurred in the period 1991–1997. Comparison with hydrological data (registered groundwater extraction and piezometric level measurements) showed that the amount of subsidence was strongly related with the amount of groundwater extraction.

The amount of land subsidence may also be estimated by comparing altitudes of high resolution DEMs, representing former and present surface topographies. Laser altimetry or radar images may be used to compute such high resolution DEMs and detect changes in surface topography (e.g., Galloway et al., 1998; Fig. 8; Table 1).

In conclusion, high-precision techniques are available to monitor surface elevation changes. Highest accuracies (mm precision) are attained by using conventional leveling, SET and differential GPS. The drawback of such techniques is that elevation changes only over short timescales are measured. Still, such surveys are useful as they give insight into the rate of processes leading to subsidence. Using high resolution DEMs and GPS surveys for surface elevation change measurements result in 10^0–10^1 cm-precision.

3.4. Deformation of logs

Rough estimates of peat compaction were made by Kaye and Barghoon (1964; Table 1), who determined the minimum amount of peat compaction from the distortion of buried logs, which were assumed to originally have been circular in cross-section. They estimated compaction of peat layers of about 25–43% of its original thickness. Stout and Spackman (1989; Table 1) used the same method and estimated minimum average compaction of peat by 21%.

This method does not give accurate estimates of the amount of peat compaction. First of all, only minimum compaction can be estimated, as probably considerable compaction of peat has taken place before flattening of the logs occurs. Furthermore, the assumption that the tree trunk and the surrounding peat have the same compressibility will introduce significant errors in the calculated amount of compaction.

4. Compaction models

Another method used to quantify the amount and rate of compaction is by the use of empirical and numerical models. Examples of such models are presented and discussed in the following sections.

4.1. Empirical models

Empirical models are based on results from experiments and observations. Empirical compaction models are often based on porosity–depth relations. There are numerous porosity–depth equations, but it is not the aim of this paper to review all of these, especially since many of these equations were constructed for (deep buried) clastic sediments and not for peat. Some that do account for compaction of peat are discussed here.

Sheldon and Retallack (2001) developed a porosity–depth equation for nonmarine sediments such as floodplain sediments and peat. This equation was based on porosity–depth equations for deep buried sediments of Sclater and Christie (1980) and of Baldwin and Butler (1985):

$$C = \frac{-S_i}{\left(\left(F_0/e^{Dk}\right)-1\right)}, \tag{2}$$

where C is the compaction as a fraction of the original thickness, S_i is the initial solidity ($=1-F_0$), F_0 is the initial porosity, D is the burial depth and k is an empirically derived constant. Values for k were determined using empirical relationships with the initial porosity, valid for marine sediments (Sclater and Christie, 1980). Thus, a required parameter in this model is the initial solidity of the sediment under consideration, which was calculated using the dry bulk density and the solid bulk density. Sheldon and Retallack (2001) used $S_i=0.06$ ($F_0=0.94$) and $k=2.09$ to calculate compaction of peat. Using these values, the compaction ratio becomes 0.85 at 5 meter and 0.75 at 10 meter depth (85% and 75% respectively of the original thickness).

Allen (1999) used a simple empirical equation, based on experimental research of Skempton (1970), to estimate the amount of compaction in coastal mudflats and marshes:

$$T = (T_0 - T_{\min})e^{-kH} + T_{\min}, \tag{3}$$

where T is the final thickness of a sediment layer, T_0 the thickness at the time of deposition, $T_{\min}$ the limiting thickness (zero porosity), k the empirical compressibility of the layer, and H the thickness of the sediment overburden, assumed to fill the accommodation space to the height determined by sea level at that time. Values of k for each type of sediment were estimated by solving the formula with field data. A bulk density for the initial and most compacted state was assumed to estimate T_0 and $T_{\min}$ respectively. To quantify the effect of accommodation space provided by compaction on deposition rate, the deposition-rate enhancement factor (*DEF*) was used:

$$DEF = \frac{\Delta S_{\min} + \Delta S_{\text{org}}}{\Delta M} = 1 + \frac{\Delta P}{\Delta M}, \tag{4}$$

where $\Delta S_{\min}$ is the added thickness of mineral sediment, ΔS_{org} the thickness of organic material, ΔM the change in relative sea level and ΔP the lowering of the surface due to compaction. Thus, following this equation, changes in accommodation space are determined by changes in sea level (or another local base level) and by compaction. Assuming a steady sea level rise of 1.5 mm/yr, the *DEF* gradually increases in a

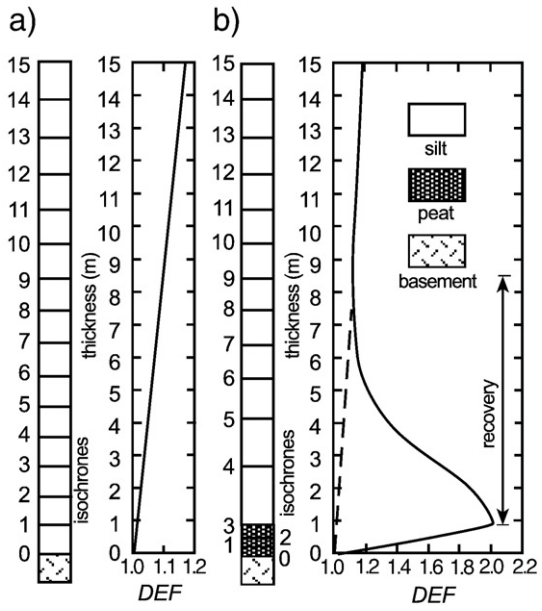

Fig. 16. The deposition-rate enhancement factor (*DEF*) used to quantify the effect of accommodation space provided by compaction on deposition rate. In (a) the *DEF* gradually increases in a sequence formed over 15 periods of silt deposition (one period equals 667 years). (b) shows the effect of 3 periods of peat accumulation followed by 12 periods of silt deposition. The *DEF* first rapidly increases due to high rate of creation of accommodation space by peat compaction. Continued peat compaction enhances silt deposition, but after about 6 periods the *DEF* has recovered again. After Allen (1999).

sequence formed over 15 periods of silt deposition (Fig. 16a; one period equals 667 years). In Fig. 16b 3 periods of peat accumulation are followed by 12 periods of silt deposition. In this case, the *DEF* first rapidly increases due to high rate of creation of accommodation space by peat compaction. Continued peat compaction enhances silt deposition, but after about 6 periods the *DEF* has recovered again.

Fokkens (1970) set up an empirical relation based on compression tests on a large number of peat samples. Using an empirical relation between the organic matter content and the specific gravity of the solids (Den Haan and Amir, 1994) the following empirical equation was used to estimate the amount of settlement:

$$\frac{\Delta h}{h} = \frac{w_i - w_u}{w_i + n + mN}, \tag{5}$$

where Δh is the amount of subsidence (m), h is the initial layer thickness (m), w_i is the initial water content, w_u is moisture content after compression, N is the organic matter content (determined by LOI test; N = weight organic matter in soil sample / weight solid fraction of soil sample) and m and n are fitted parameters (see also Kruse, 1998).

4.2. Geotechnical models

Most compaction models however, are based on geotechnical theory, which basically describes stresses occurring in soil. The most important law used in such models is Terzaghi's principle of effective stress (σ'), which is the stress between soil particles (Eq. 1). Different kinds of geotechnical compaction models exist: models that only describe one-dimensional (vertical) compression, three-dimensional models, models describing consolidation (pore water expulsion), models that distinguish between primary and secondary compression. Furthermore, a distinction can be made between backward and forward modeling. A backward modeling approach starts from the compacted state and estimates the decompaction correction. A forward modeling approach calculates the amount of compaction starting from the uncompacted state.

4.2.1. Models describing one-dimensional compression

Many compaction models describe only one-dimensional (vertical) compression, and are based on Terzaghi's law (Eq. 1). Necessary model parameters, such as compression coefficients (slope of stress/strain curve; see Section 1.4), are often determined with oedometer tests.

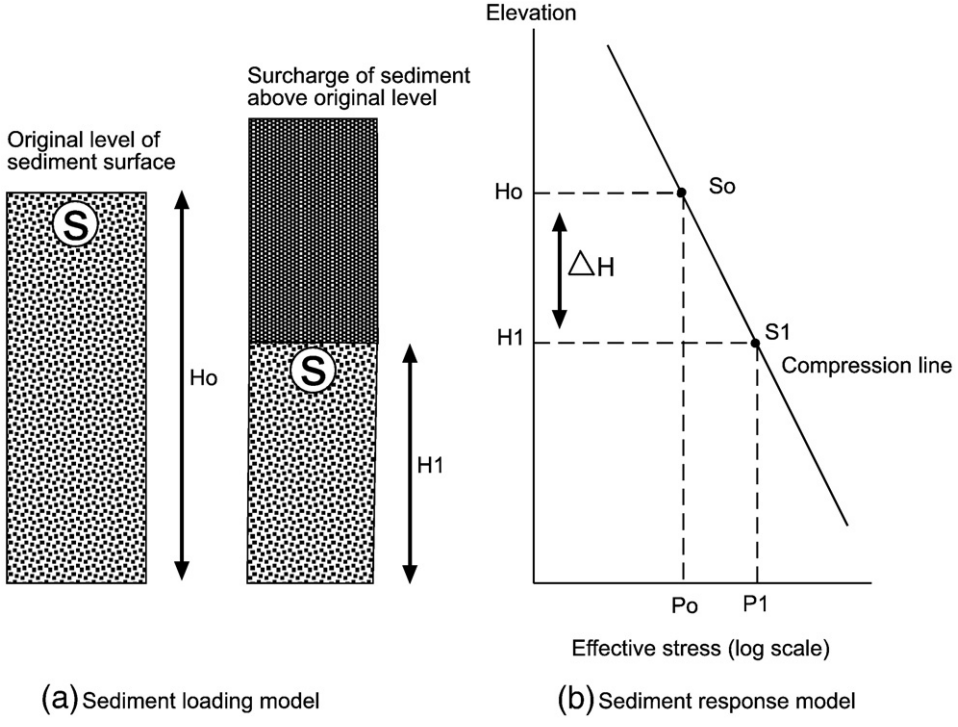

Fig. 17. Calculating the decompacted thickness of a sediment layer after the model of Paul and Barras (1998). The original height H_0 of a sample S is lowered to height H_1, after an increase of the effective stress from P_0 to P_1, due to the load of the added sediment layer. ΔH depends on the ratio of effective stresses (P_0 to P_1) and the slope of the compression line (=compression index).

Table 2
Range of values for primary (suffix p) and secondary (suffix s) compression coefficients of Buisman–Koppejan, for conditions before and after the preconsolidation stress (suffix 1 and 2 respectively; from Locher and de Bakker, 1993)

Soil type	C_{p1}	C_{s1}	C_{p2}	C_{s2}
Peat	10–150	25–1000	4–30	14–140
Clay	20–300	60–2500	7–125	30–300
Sand	80–800	70–3500	140–140	40–1250

For example, Paul and Barras (1998) developed a simple one-dimensional compression model, using a backward modeling approach (Fig. 17). Massey et al. (2006) used the same model to calculate the decompaction correction for 10 to 15 m thick Holocene sediments in southern UK. In the model, the sediment sequence is first divided into layers of 0.1–0.2 m thick, for each of which the volume reduction is calculated according to the stress increase the layer has experienced. The total subsidence due to compaction is the sum of these volume changes. Fig. 17 shows that the increase in effective stress (P_0 to P_1) following sediment loading, causes subsidence of sample S of ΔH. The effective stress was calculated based on Terzaghi's law of effective stress (Eq. 1), for which the pore water pressure was calculated from the depth of a sample below the water table (assumed 1 m below surface) and the total stress was calculated based on the weight and thickness of the sequence overlying the sample. As outlined before, peat may show a high variability concerning its geotechnical characteristics. Consequently, it may be difficult to determine the compression index from oedometer tests. Therefore, the compression index (slope of the compression line in Fig. 17b) of peat was calculated using a correlation with the liquid limit (the water content at which a soil changes from a liquid state to a plastic state). However, the relation used was originally derived from results from mineralogenic sediments (Skempton, 1944), which therefore introduced a significant uncertainty into the model calculations.

Other one-dimensional compaction models also describe fluid flow. Groundwater flow in porous sediments is usually modeled assuming Darcy's law, in which flow velocity is a function of the permeability of the sediment and of the gradient of the water table. Furthermore, besides assuming Terzaghi's law of effective stress (Eq. 1), changes in effective stress are often modeled using porosity-effective stress relations (e.g., Kooi, 1997; Kooi and De Vries, 1998; Meckel et al., 2007), or using void-ratio-effective stress relations (Audet, 1996; Pizzuto and Schwendt, 1997; Tovey and Paul, 2002; Gutierrez and Wangen, 2005). Void ratio is defined as the ratio between the volume of voids and the volume of solids. Oedometer tests show that the void ratio is linearly related to the logarithm of the effective vertical stress (Skempton, 1944):

$$\sigma'_v = \sigma_{100} \exp_{10}\left(\frac{e_{100}-e}{C_c}\right), \qquad (6)$$

$$e_{100}-e = C_c\frac{\ln\sigma_{'v}}{\ln\sigma_{100}}$$

where, σ_{100} is a reference value for σ'_v (usually 100 kPa), e_{100} is the void ratio at σ'_v = 100 kPa and C_c is the compression index.

Based on calculations used in the model of Kooi (1997), Meckel et al. (2007) used a forward modeling approach to model sedimentation and subsequent compaction rates of stochastically generated sediment sequences with different thicknesses, sedimentation rates and lithologic composition. Highest compaction rates were found in stratigraphies with a high proportion of peat layers that are loaded with high bulk density lithologies such as sand.

Table 3
Values for compression parameters resulting from 7 oedometer tests on peat samples taken from western Netherlands (Kruse, 2004)

	C_{p1}	C_{s1}	C_{p2}	C_{s2}
Average	19.52	110.85	5.08	26.30
Maximum	24.01	210.40	5.61	43.18
Minimum	12.33	48.98	4.43	13.05

4.2.2. Three-dimensional models

In environments that are severely influenced by tectonics or by increased stresses resulting from artificial constructions such as dykes, lateral deformations can be important (e.g., Lefebvre et al., 1984). To model three-dimensional deformation in deep buried fine-grained sedimentary basins, Pouya et al. (1998) introduced a mechanical constitutive model. In Holocene peatlands in deltaic settings however, lateral strain will be of minor importance compared to vertical strain.

4.2.3. One-dimensional models describing primary and secondary compression

Secondary compression was not considered in previous mentioned models. Especially in peat however, secondary compression causes a considerable part of total compaction, and therefore should be taken into account.

Terzaghi (1943) described primary and secondary compression with the following equation:

$$s = h\frac{C_c}{1+e_0}\log\frac{\sigma'_v+\Delta\sigma'_v}{\sigma'_v} + hC_\alpha \log t \qquad (7)$$

where s is the settlement (Δh), h is the layer thickness, C_c the primary compression index, e_0 the initial void ratio, C_α the secondary compression index and t the time in days. The second term ($hC_\alpha \log t$) describes secondary settlement, which is independent of the vertical stress and occurs after the hydrodynamic period has ended.

Contrary, in the model of Buisman–Koppejan (described in Den Haan, 2003) secondary compression is dependent on the effective stress. It is assumed that primary and secondary compression both start directly after loading. Compression is calculated using the equation:

$$s = h\left(\frac{1}{C_p}+\frac{1}{C_s}\log t\right)\ln\frac{\sigma'_v+\Delta\sigma'_v}{\sigma'_v} \qquad (8)$$

where C_p and C_s are the primary and secondary compression coefficients of Buisman–Koppejan respectively. In this model, the rate of secondary compression (settlement) is dependent on previous

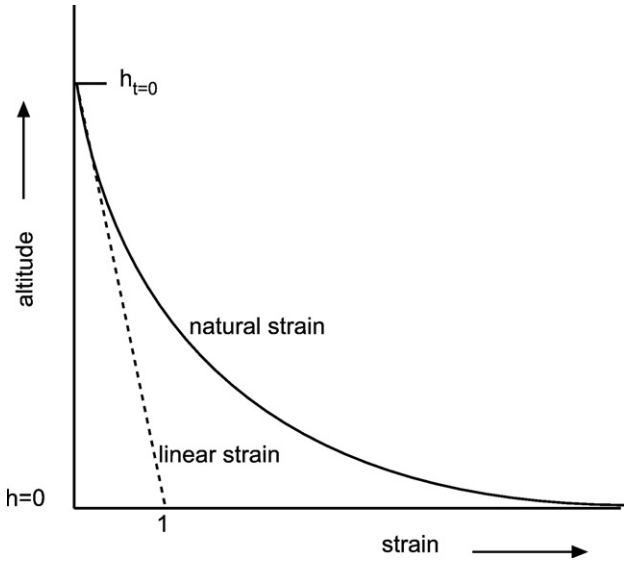

Fig. 18. Graphical interpretation of linear and natural strain (from Den Haan, 1994).

effective stress increases ('superposition rule'). Ranges of values for C_p and C_s for three types of soil are presented in Table 2. Mean values resulting from oedometer tests on peat samples from the western part of The Netherlands, taken from different depths (Kruse, 2004) are shown in Table 3.

However, it appeared from long duration compression tests that the secondary compression rate was not dependent on the effective stress after all. Actually, Bjerrum (1967) already found that creep (=secondary compression)-strain rates are constant in a plot of strain versus the natural logarithm of vertical effective stress. Such lines are called creep isotaches. The *a–b–c isotach model* uses this concept and was developed by Den Haan (1994) to improve modeling of compaction of soft soils like peat. In this model, natural strain (ε^H) instead of linear strain (ε^C) is used to better describe large compressions. For large compressions, ε^C tends to 1, but ε^H tends to infinity (Fig. 18). Natural strain is described as:

$$\varepsilon^H = -\int_{h=h_0}^{h=h} \frac{-dh}{h} = -\ln\frac{h}{h_0} = -\ln(1-\varepsilon^c) \tag{9}$$

Natural strain is incrementally defined, whereas linear strain is a differential measure. Above approximately 10% compression the difference between linear and natural strain becomes noticeable, and therefore in highly compressible soils like peat, the use of natural strain is of advantage (Den Haan and Edil, 1993).

Another difference with most other compaction models is that the *a–b–c isotach model* uses intrinsic time. Intrinsic time is described as the time which would have been necessary to achieve the present volume, assuming that the present stress had been applied immediately to the soil in its freshly deposited state (Den Haan and Edil, 1993). Intrinsic time (τ) is defined as:

$$\tau = t - t_r \tag{10}$$

where t_r is a time constant. In the *a–b–c isotach* model, three main parameters are used (*a*, *b* and *c*) to describe soil compressibility

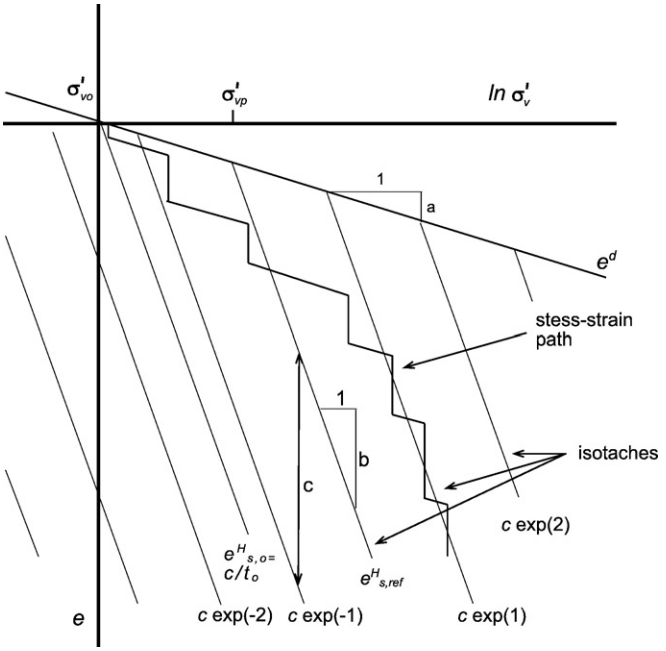

Fig. 19. Stress–strain–creep strain rate relationships according the a–b–c-isotach model (Den Haan, 1994). Creep isotaches are shown with slope *b* and vertical distance *c*. Initial conditions are represented by effective stress σ'_{vo} with creep strain rate $\dot{\varepsilon}^s_o$. The line representing direct compression (ε^d) has slope gradient *a*. σ'_{vp} is the preconsolidation stress. See text for further explanation.

Table 4
Values for compression parameters *a*, *b* and *c* used in the a,b,c-isotach model, derived from compression tests on peat samples taken from different depths (Kruse, 2004)

	a	*b*	*c*
Mean	0.062	0.32	0.022
Maximum	0.083	0.34	0.034
Minimum	0.044	0.30	0.013

(Fig. 19). Direct compression, following an increase in effective stress, is described by parameter *a*:

$$\varepsilon^H_d = a\ln\left(\frac{\sigma'_v}{\sigma'_{vp}}\right) \tag{11}$$

The slope of the creep isotaches as shown in Fig. 19 is given by parameter *b*. The vertical distance between two lines is given by parameter *c* if their rates differ by a factor exp(1). The reference isotach starts at the preconsolidation stress (σ'_{vp}) and is characterized by a reference creep strain rate $\dot{\varepsilon}^H_{s,ref}$. The creep isotaches are described by:

$$\dot{\varepsilon}^H_s = \dot{\varepsilon}^H_{s,ref}\exp\left(\frac{(b-a)\ln\left(\frac{\sigma'}{\sigma'_{vp}}\right)-\varepsilon^H_s}{c}\right) \tag{12}$$

The creep rate is related to the intrinsic time by:

$$\dot{\varepsilon}^H_s = \frac{c}{\tau} \tag{13}$$

Total rate of strain is calculated using:

$$\dot{\varepsilon}^H = \dot{\varepsilon}^H_d + \dot{\varepsilon}^H_s \tag{15}$$

Values for parameters *a*, *b*, and *c* resulting from tests on peat samples taken from western Netherlands (Kruse, 2004) are presented in Table 4. These values correspond with other values found in literature (Den Haan, 1994).

The model takes into account reduced pore volume during consolidation, leading to reduced permeability and increased stiffness of the soil. The outflow of pore water is modeled using Darcy's law.

4.3. Discussion peat compaction models

According to Den Haan (2003), the a,b,c-isotach model is currently most realistic for modeling compaction of soft soils like peat as it 1) takes into account secondary compression, 2) uses natural strain instead of linear strain, which better describes large compressions in soft soils, and 3) creep rate is a function of effective stress and strain.

The model can still be improved however, as for example stress distributions in soil are not accurately described, which is necessary though when describing e.g., lateral stresses occurring as a result of artificial constructions. Currently, the model uses Boussinesq's (1885) theory to describe stresses in soil, in which a linear relationship between the applied stress and the resulting strain is assumed using the Poisson ratio. In the plain of the maximum vertical and minimum horizontal applied stress, this parameter is defined as the ratio between the strain in vertical direction to the strain in horizontal direction. Boussinesq's theory assumes that the soil is an isotropic, homogenous linear elastic material, and that the stress distribution is the same in different soil types. Soils however rarely meet these conditions, and stress distributions will vary between different soil types. For example, considering natural levee and crevasse splay deposits next to a channel belt, the vertical effective stress will be highest close to the channel where the levee is thickest, and the

applied stress will distribute differently through the sand of the channel and the floodplain deposits (peat and clay).

Besides choosing the most suitable compaction model, another difficulty in modeling peat compaction is to determine the highly variable geotechnical characteristics of peat (Magnan, 1993; Termaat and Topolnicki, 1993). This is the result of a combination of factors, such as the type of organic material (e.g., wood, sedge or reed peat), clastic content and the chemical and biological evolution of the organic matter with time (degree of decomposition).

To overcome the problem of determining compression parameters of peat samples, Paul and Barras (1998) and Massey et al. (2006) used a relation between the compression index and the liquid limit. This correlation usually underestimates the compression index for very soft materials and will probably vary between different peat types. Pizzuto and Schwendt (1997) also stressed that their organic samples could not be used in oedometer tests due to the high contents of large organic debris (e.g., wood fragments). They estimated model parameters for organic deposits by model calibration. However, parameters obtained from model calibration are not very reliable as different combinations of parameters may lead to the same results.

Another solution to take into account the variability of peat is using relatively large samples in oedometer tests, as larger samples are representative for a larger volume of peat soil. Normally, samples of about 6 cm in diameter and 2 cm in height are used. For peat, samples of about 20 cm in diameter and 8 cm in height might give more reliable results. A disadvantage of using larger samples in oedometer tests is that it takes much longer before all pore water is expelled (long consolidation time), so testing will be more time-consuming (Lefebvre et al., 1984).

4.3.1. Peat compaction in alluvial architecture models

Alluvial architecture models are used by geologists and reservoir engineers to understand and predict the spatial distribution and geometry of (sandy) channel belts (e.g., Leeder, 1978; Bridge and Leeder, 1979; Mackey and Bridge, 1995; Karssenberg and Bridge, 2008). Until now, compaction processes are not, or only in a simplified from, incorporated in such models. In the two-dimensional process-based alluvial architecture model of Bridge and Leeder (1979) fine-grained overbank deposits are compacted using a polynomial equation based on porosity–depth curves of Baldwin (1971) and Rieke and Chilingarian (1974; Fig. 20). However, these porosity–depth curves were based on data derived from marine sediments, which may not be applicable to alluvial sediments, and especially not to peat. Mackey and Bridge (1995) used a different expression to simulate porosity changes with depth, allowing for higher near-surface porosities, and for a faster porosity reduction near the surface (Alternate Shale Curve in Fig. 20).

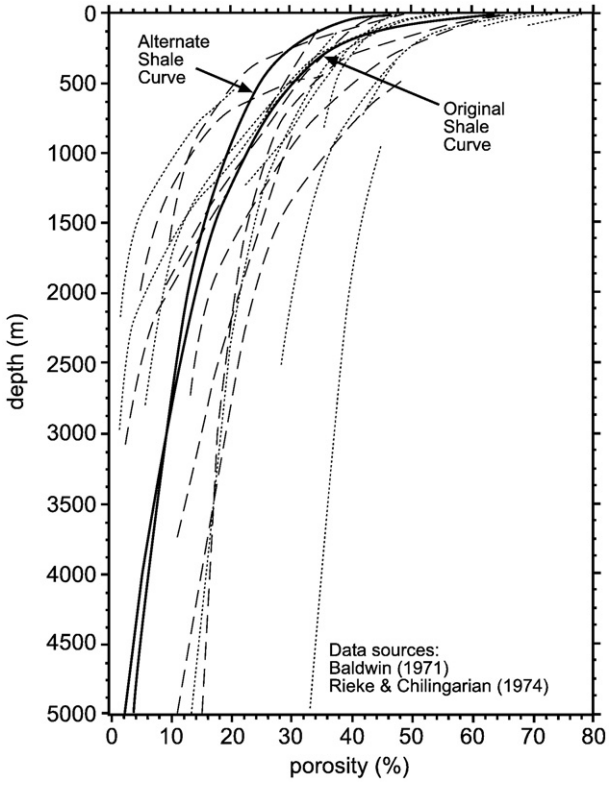

Fig. 20. Porosity–depth curves, with data from Baldwin (1971; short dashed lines) and Rieke and Chilingarian (1974; long dashed lines). The Original Shale Curve is the best fit to these data. The Alternate Shale Curve more closely approximates the rapid loss of porosity near the surface in alluvial sediments (Anderson, 1991, in: Mackey and Bridge, 1995).

Many Holocene deltas comprise peat, which is highly sensitive to compaction and thereby influences alluvial architecture, as is outlined in this paper. Present alluvial architecture models can be greatly improved by incorporating peat compaction and peat formation. For modeling peat compaction it is suggested to use the a,b,c-isotach model as a basis for reasons mentioned above. Initially, peat formation in an aggrading system can simply be modeled by assuming it keeps up with the groundwater table rise.

Including peat compaction and formation might for example affect the ratio between cross-valley (s_{cv}) and down-valley (s_{dv}) gradient, which is often used in alluvial architecture models as an important factor controlling the occurrence of avulsion (e.g., Mackey and Bridge, 1995; Karssenberg and Bridge, 2008). Although it has been proved that this is not the only control on avulsion (Aslan et al., 2005; Stouthamer and Berendsen, 2007), some suggestions were made in Section 2 about how peat formation and compaction affect this ratio. However, considering a situation of groundwater table rise, as is common in most Holocene deltas, the s_{cv}/s_{dv} ratio will not increase as long as peat formation in the flood basin can keep up with the rise of the water table. When peat bogs develop further away from the river, the ratio might even decrease. Furthermore, peat compaction underneath fluvial deposits initially leads to subsidence, thereby creating accommodation space for increased fluvial deposition. If sedimentation rate keeps up with subsidence due to peat compaction, it is thought the s_{cv}/s_{dv} ratio will not greatly alter. Overall, it is thought that incorporating peat compaction and formation into alluvial architecture models will decrease avulsion probability. In such environments avulsions most likely occur due to random crevassing during periods of high discharge.

5. Conclusions

Peat compaction and formation are key processes in delta evolution, especially in distal parts with relatively high accommodation rates where thick peat layers are formed in the flood basins. The way and magnitude by which peat compaction and formation influence delta architecture strongly depend on temporal and spatial scale. Peat compaction and formation influence the following aspects of delta evolution:

1) Channel belt elevation. In a situation of groundwater table lowering, subsidence due to compaction and oxidation of peat above the groundwater table in flood basins leads to relief amplification of sandy channel belts or inversion of former creeks filled with sand. Relief amplification might lead to avulsion.
2) Channel belt geometries. Vertical aggradation, resulting in channel belts with low width/depth ratios, is favored by I) the high cohesiveness of peat inhibiting bank erosion and II) peat compaction underneath a channel belt creating accommodation space for fluvial deposition. Contrary, if a relatively thin peat layer is intercalated in between less cohesive sediments, an incising channel will first erode to the depth of the peat layer, which due to its high resistance prevents further vertical incision resulting in channels belts with a high width/depth ratio.

3) Channel belt configuration and distribution of fluvial deposits. A decrease in the rate of accommodation space created by peat compaction underneath a channel belt increases the tendency for lateral migration and hence, the channel becomes more prone to avulsion. The combination of a high bank stability, low regional gradients and low stream power in peatlands favors crevassing, which is an important mechanism initiating avulsion. At a larger scale, invasion of a river system onto a new part of a floodplain is stimulated by I) variations in compaction rate across a floodplain and II) a sudden drop in gradient a river experiences where it enters a peatland causes higher rates of clastic deposition at the edges of peatlands, which stimulates the occurrence of nodal avulsions.

The third mentioned aspect is still mainly a hypothesis. The influence of peat compaction and formation on delta evolution is influenced by many factors such as peat type, organic matter content, sediment sequence composition and ground water table fluctuations, which so far are seldom taken into account. To determine the relative importance of these factors and to quantify the influence of peat compaction and formation on different aspects of delta evolution field research should be combined with numerical models describing peat compaction and formation. To calibrate and validate such a model field data is needed, including lithological data, time control, and groundwater table reconstructions, all at delta scale. The Rhine–Meuse delta dataset contains this kind of data and therefore would be a suitable dataset for calibration and validation.

Acknowledgements

This paper greatly benefited from the critical and constructive reviews by Whitney Autin and Marta Pérez-Arlucea. We thank Ward Koster, Kim Cohen and Hans Middelkoop for commenting on earlier drafts of this paper. Henk Kruse and Gerard Kruse (GeoDelft/Deltares) are thanked for explaining the *a–b–c isotach* model of Den Haan (1994). This research was funded by the Netherlands Organization for Scientific Research — Earth and Life Sciences (NWO-ALW, project 814.01.014) and Utrecht University, Faculty of Geosciences.

References

Abidin, H.Z., Djaja, R., Darmawan, D., Hadi, S., Akbar, A., Rajiyowiryono, H., Sudibyo, Y., Meilano, I., Kasuma, M.A., Kahar, J., Subarya, C., 2001. Land subsidence of Jakarta (Indonesia) and its geodetic monitoring system. Natural Hazards 23, 365–387.

Allen, J.R.L., 1978. Studies in fluviatile sedimentation: an exploratory quantitative model for the architecture of avulsion-controlled alluvial suites. Sedimentary Geology 21, 129–147.

Allen, J.R.L., 1999. Geological impacts on coastal wetland landscapes: some general effects of sediment autocompaction in the Holocene of northwest Europe. The Holocene 9, 1–12.

Allen, J.R.L., 2000. Holocene coastal lowlands in NW Europe: autocompaction and the uncertain ground. In: Pye, K., Allen, J.R. (Eds.), Coastal and Estuarine Environments: sedimentology, geomorphology and geoarchaeology. Special Publication — Geological Society of London, vol. 175, pp. 239–252.

Amorosi, A., Milli, S., 2001. Late Quaternary depositional architecture of Po and Tevere river deltas (Italy) and worldwide comparison with coeval deltaic successions. Sedimentary Geology 144, 357–375.

Anderson, S., 1991. differential compaction in alluvial sediment (unpublished PhD. Thesis), University of Wales, Cardiff, Wales, 199 pp.

Aslan, A., Autin, W.J., Blum, M.D., 2005. Causes of river avulsion: insights from the Late Holocene avulsion history of the Mississippi River, U.S.A. Journal of Sedimentary Research 75, 648–662.

Audet, D.M., 1996. Compaction and overpressuring in Pleistocene sediments on the Louisiana Shelf, Gulf of Mexico. Marine and Petroleum Geology 13, 467–474.

Baldwin, B., 1971. Ways of deciphering compacted sediments. Journal of Sedimentary Petrology 41, 293–301.

Baldwin, B., Butler, C.O., 1985. Compaction curves. American Association of Petroleum Geologists Bulletin 69, 622–626.

Berendsen, H.J.A., 2000. Landschap in delen. Overzicht van de geofactoren. Fysische geografie van Nederland, 2nd edition. Van Gorcum, Assen (in Dutch).

Berendsen, H.J.A., 2005. Landschappelijk Nederland, De fysisch-geografische regio's. Fysische Geografie van Nederland, 3rd edition. Van Gorcum, Assen (in Dutch).

Berendsen, H.J.A., Vollenberg, K.P., 2007. New prospects in geomorphological and geological mapping of the Rhine–Meuse Delta — application of detailed digital elevation maps based on laser altimetry. Netherlands Journal of Geosciences 86 (1), 15–22.

Beuving, J., van den Akker, J.J.H., 1996. Maaiveldsdaling van veengrasland bij twee slootpeilen in de polder Zegvelderbroek. Vijfentwintig jaar zakkingsmetingen op het ROC Zegveld. Rapport, vol. 377. DLO-Staring Centrum, Wageningen (in Dutch).

Bird, M.I., Fifield, L.K., Chua, S., Goh, B., 2004. Calculating sediment compaction for radiocarbon dating of intertidal sediments. Radiocarbon 46, 421–435.

Bjerrum, L., 1967. Engineering geology of Norwegian normally-consolidated marine clays as related to settlements of buildings. Geotechnique 17, 81–118.

Bloom, A.L., 1964. Peat accumulation and compaction in a Connecticut coastal marsh. Journal of Sedimentary Petrology 34, 599–603.

Boussinesq, J., 1885. Application des potentiels à l'étude de l'équilibre et du mouvement des solides élastiques. Gauthier-Villars, Paris. 30 pp.

Boumans, R., Day Jr., J.W., 1993. High precision measurements of sediment elevation in shallow coastal areas using a sedimentation–erosion table. Estuaries 16, 375–380.

Brandyk, T., Szatylowicz, J., Oleszczuk, R., Gnatowski, T., 2002. Water-related physical attributes of organic soils. In: Parent, L.E., Ilnicki, P. (Eds.), Organic soils and peat materials for sustainable agriculture. CRC Press, LLC, US.

Bridge, J.S., Leeder, M.R., 1979. A simulation model of alluvial stratigraphy. Sedimentology 26, 617–644.

Buisman, A.S.K., 1940. Grondmechanica. 294 pp. Reprinted by Balkema, 1996.

Buttler, A., Grosvernier, P., Matthey, Y., 1998. A new sampler for extracting undisturbed surface peat cores for growth pot experiments. New Phytologist 140, 155–160.

Cahoon, D.R., Reed, D.J., Day, J.J.W., 1995. Estimating shallow subsidence in microtidal salt marshes of the southeastern United States: Kaye and Barghoon revisited. Marine Geology 128, 1–9.

Cahoon, D.R., Marin, P.E., Black, B.K., Lynch, J.C., 2000. A method for measuring vertical accretion, elevation, and compaction of soft, shallow-water sediments. Journal of Sedimentary Research 70, 1250–1253.

Charman, D.J., 2002. Peatland systems and environmental change. John Wiley & Sons, Chichester. 301 pp.

Chen, C., Pei, S., Jiao, J.J., 2003. Land subsidence caused by groundwater exploitation in Suzhou City, China. Hydrogeology Journal 11, 275–287.

Clari, P.A., Martire, L., 1996. Interplay of cementation, mechanical compaction, and chemical compaction in nodular limestones of the Rosso Ammonitico Veronese (Middle-upper Jurassic, northeastern Italy). Journal of Sedimentary Research 66 (3), 447–458.

Craig, R.F., 1987. Soil Mechanics, Fourth Edition. Van Nostrand Reinhold (International).

Den Haan, E.J., 1994. Vertical compression of soils. Delft University, Thesis.

Den Haan, E.J., 2003. Het a,b,c-isotachenmodel: Hoeksteen van een nieuwe aanpak van zettingsberekeningen. Geotechniek 28–35 oktober (in Dutch).

Den Haan, E.J., Amir, L.S.F., 1994. A simple formula for final settlement of surface loads on peat. International workshop "Advances in understanding and modelling the mechanical behaviour of peat", June 16–18, 1993, Delft, The Netherlands.

Den Haan, E.J., Edil, T.B., 1993. Secondary and tertiary compression of peat. International workshop "Advances in understanding and modelling the mechanical behaviour of peat", June 16–18, 1993, Delft, The Netherlands.

Ericson, J.P., Vorosmarty, C.J., Dingman, S.L., Ward, L.G., Meybeck, M., 2006. Effective sea-level rise and deltas: Causes of change and human dimension implications. Global and Planetary Change 50, 63–82.

Fokkens, B., 1970. Berekening van de samendrukking van veenlagen uit het gehalte aan organische stof en water. De ingenieeur, Bouw- en waterbouwkunde, vol. 3, pp. 1–20.

Galloway, D.L., Hudnut, K.W., Ingebritsen, S.E., Phillips, S.P., Peltzer, G., Rogez, F., Rosen, P.A., 1998. Detection of aquifer system compaction and land subsidence using interferometric synthetic aperture radar, Antelope Valley, Mojave Desert, California. Water Resources Research 34, 2573–2585.

Gambolati, G., Putti, M., Teatini, P., Gasparetto Stori, G., 2006. Subsidence due to peat oxidatio and impact on drainage infrastructures in a farmland catchment south of the Venice Lagoon. Environment Geology 49, 814–820.

GeoDelft, 2003. Geotechnics, working lectures practical work visit, project number 450050. In: Brinkman, J., Kruse, G.A.M., Dillingh, D.A., Kruse, H.M.G. (Eds.), GeoDelft, march 2003.

Givelet, N., Le Roux, G., Cheburkin, A., Chen, B., Frank, J., Goodsite, M.E., Kempter, H., Krachler, M., Noernberg, T., Rausch, N., Rhuinberger, S., Roos-Barraclough, F., Sapkota, A., Scholz, C., Shotyk, W., 2004. Suggested protocol for collecting, handling and preparing peat cores and peat samples for physical, chemical, mineralogical and isotopic analyses. Journal of Environmental Monitoring 6, 481–492.

Gouw, M.J.P., 2007. Alluvial architecture of fluvio-deltaic successions: a review with spherical reference to Holocene settings. In: Middelkoop, H., Stouthamer, E., Hoek, W.Z. (Eds.), Geomorphology and Climate — In honour of Professor dr. Eduard A. Koster. Netherlands Journal of Geosciences, vol. 86, pp. 211–227.

Gouw, M.J.P., Berendsen, H.J.A., 2007. Variability of channel-belt dimensions and the consequences for alluvial architecture: observations from the Holocene Rhine–Meuse delta (The Netherlands and Lower Mississippi valley (U.S.A). Journal of Sedimentary Research 77, 124–138.

Gutierrez, M., Wangen, M., 2005. Modeling of compaction and overpressuring in sedimentary basins. Marine and Petroleum Geology 22, 351–363.

Haslett, S.K., Davies, P., Curr, R.H.F., Davies, C.F.C., Kennington, K., King, C.P., Margetts, A.J., 1998. Evaluating late-Holocene relative sea-level change in the Somerset Levels, southwest Britain. The Holocene 8, 197–207.

Heller, P.L., Paola, C., 1996. Downstream changes in alluvial architecture: an exploration of controls on channel-stacking patterns. Journal of Sedimentary Research 66, 297–306.

Karssenberg, D., Bridge, J.S., 2008. A three-dimensional model of sediment transport, erosion and depostion within a network of channel belts, floodplain and hillslope:

extrinsic and intrinsic controls on floodplain dynamics and alluvial architecture. Sedimentology 55 (6), 1717–1745.
Kaye, C.A., Barghoon, E., 1964. Late Quaternary sea level change and crustal rise at Bostion, Massachusetts, with notes on autocompaction of peat. Geological Society of America Bulletin 75, 63–80.
Kooi, H., 1997. Insufficiency of compaction disequilibrium as the sole cause of high pore fluid pressures in pre-Cenozoic sediments. Basin Research 9, 227–241.
Kooi, H., De Vries, J.J., 1998. Land subsidence and hydrodynamic compaction of sedimentary basins. Hydrology and Earth System Sciences 2, 159–171.
Kool, D.M., Buurman, P., Hoekman, D.H., 2006. Oxidation and compaction of a collapsed peat dome in Central Kalimantan. Geoderma 137, 217–225.
Kruse, H.M.G., 1998. Deformation of a river dyke on soft soil. Thesis, Utrecht University.
Kruse, H.M.G., 2004. Bouwrijp maken Delft Technopolis. Rapportnummer CO-410031-0008 v03. GeoDelft (in Dutch).
Latter, P.M., Howson, G., Howard, D.M., Scott, W.A., 1998. Long-term study of litter decomposition on a Pennine peat bog: which regression? Oecologia 113, 94–103.
Leeder, M.R., 1978. A quantitative stratigraphic model for alluvium, with special reference to channel deposit density and interconnectedness. In: Miall, A.D. (Ed.), Fluvial Sedimentology. Canadian Society of Petroleum Geologists Memoir, 5, pp. 587–596.
Lefebvre, G., Langlois, P., Lupien, C., Lavallée, J.G., 1984. Laboratory testing and in situ behaviour of peat as embankment foundation. Canadian Geotechnical Journal 21, 322–337.
Locher, W.P., de Bakker, H., 1993. Bodemkunde van Nederland, Deel 1, Algemene bodemkunde. (in Dutch) Malmberg, Den Bosch.
Mackey, S.D., Bridge, J.S., 1995. Three-dimensional model of alluvial stratigraphy: theory and application. Journal of Sedimentary Research. Section B, Stratigraphy and Global Studies 65, 7–31.
Magnan, J.P., 1993. Construction on peat: state of the art in France. Proceedings of International Workshop on Advances in understanding and modelling the mechanical behaviour of peat, April 1993.
Makaske, B., 1998. Anastomosing rivers. Forms, processes and sediments. Thesis. Utrecht University.
Makaske, B., 2001. Anastomosing rivers: a review of their classification, origin and sedimentary products. Earth-Science Reviews 53 (3–4), 149–196.
Massey, A.C., Paul, M.A., Gehrels, W.R., Charman, D.J., 2006. Autocompaction in Holocene coastal back-barrier sediments from south Devon, southwest England, UK. Marine Geology 226, 225–241.
Meckel, T.A., Ten Brink, U.S., Williams, S.J., 2007. Sediment compaction rates and subsidence in deltaic plains: numerical constraints and stratigraphic influences. Basin Research 19 (1), 19–31.
Michaelsen, P., Henderson, R.A., Crosdale, P.J., Mikkelsen, S.O., 2000. Facies architecture and depositional dynamics of the Upper Permian Rangal Coal Measures, Bowen Basin, Australia. Journal of Sedimentary Research 70, 879–895.
Morozova, G.S., Smith, N.D., 2000. Holocene avulsion styles and sedimentation patterns of the Saskatchewan River, Cumberland marshes, Canada. Sedimentary Geology 130, 81–105.
Paul, M.A., Barras, B.F., 1998. A geotechnical correction for post-depositional sediment compression: examples from the Forth Valley, Scotland. Journal of Quaternary Science 13, 171–176.
Pizzuto, J.E., Schwendt, A.E., 1997. Mathematical modeling of autocompaction of a Holocene transgressive valley-fill deposit, Wolfe Glade, Delaware. Geology 25, 57–60.
Pouya, A., Djeran-Maigre, I., Lamoureux-Var, V., Grunberger, D., 1998. Mechanical behaviour of fine grained sediments: experimental compaction and three-dimensional constitutive model. Marine and Petroleum Geology 15, 129–143.
Price, J.S., Cagampan, J., Kellner, E., 2005. Assessment of peat compressibility: is there an easy way? Hydrological Processes 19, 3469–3475.
Rajchl, M., Uličný, D., 2005. Depositional record of an avulsive fluvial system controlled by peat compaction (Neogene, Most Basin, Czech Republic). Sedimentology 52, 601–626.
Rieke, H.H., Chilingarian, G.V., 1974. Compaction of argillaceous sediments. Developments in Sedimentology, vol. 16. Elsevier, Amsterdam. 424 pp.
Rijkswaterstaat-AGI, 2005. (in Dutch) Actueel Hoogtebestand van Nederland. Revised version. Rijkswateraat, Adviesdienst Geo-infomratie en ITC, Delft.
Rodolfo, K.S., Siringan, F.P., 2006. Global sea-level rise is recognised, but flooding from anthropogenic land subsidence is ignored around northern Manila Bay, Philippines. Disasters 30, 118–139.
Rogers, K., Saintilan, N., 2006. Vegetation change and surface elevation dynamics in estuarine wetlands of southeast Australia. Estuarine, Coastal and Shelf Science 66, 559–569.
Schothorst, C.J., 1977. Subsidence of low moor peat soils in the western Netherlands. Geoderma 17, 265–291.
Sclater, J.G., Christie, P.A.F., 1980. Continental stretching: explanation of post-mid-Cretaceous subsidence of the central North Sea Basin. Journal of Geophysical Research 85, 3711–3939.
Sheldon, N.D., Retallack, G.J., 2001. Equation for compaction of paleosols due to burial. Geology 29, 247–250.
Shennan, I., Horton, B., 2002. Holocene land-and sea-level changes in Great Britain. Journal of Quaternary Science 17, 511–526.
Skempton, A.W., 1944. Notes on compressibility of clays. Quaternary Journal Geological Society of London 100, 119–135.
Skempton, A.W., 1970. The consolidation of clays by gravitational compaction. Quarternary Journal of the Geological Society of London 125, 373–411.
Smith, N.D., Pérez-Arlucea, M., 2004. Effects of peat on the shapes of alluvial channels: examples from the Cumberland Marshes, Saskatchewan, Canada. Geomorphology 61, 323–335.
Smith, N.D., Cross, T.A., Dufficy, J.P., Clough, S.R., 1989. Anatomy of an avulsion. Sedimentology 36, 1–23.
Spijker, J., 2005. Geochemical patterns in the soils of Zeeland. Netherlands Geographical Studies 330/KNAG, Utrecht.
Stout, S.A., Spackman, W., 1989. Notes on the compaction of a Florida peat and the Brandon lignite as deduced from the study of compressed wood. International Journal of Coal Geology 11, 247–256.
Stouthamer, E., 2001. Holocene avulsions in the Rhine–Meuse delta, The Netherlands. PhD thesis, Netherlands Geographical Studies 283, Universiteit Utrecht, 211 pp.
Stouthamer, E., Berendsen, H.J.A., 2000. Factors controlling the Holocene avulsion history of the Rhine–Meuse delta (The Netherlands). Journal of Sedimentary Research 70, 1051–1064.
Stouthamer, E., Berendsen, H.J.A., 2007. Avulsion: the relative roles of autogenic and allogenic processes. Sedimentary Geology 198, 309–325.
Teatini, P., Ferronato, M., Gambolati, G., Gonella, M., 2006. Groundwater pumping and land subsidence in the Emilia–Romagna coastland, Italy: modeling the past occurrence and the future trend. Water Resources Research 42, 1–19.
Termaat, R., Topolnicki, M., 1993. Biaxial tests with natural and artificial peat. Proceedings of International Workshop on Advances in understanding and modelling the mechanical behaviour of peat, April 1993.
Terzaghi, K., 1943. Theoretical Soil Mechanics. John Wiley and Sons, New York.
Törnqvist, T.E., 1993. Holocene alternation of meandering and anastomosing fluvial systems in the Rhine–Meuse Delta (central Netherlands) controlled by sea-level rise and subsoil erodibility. Journal of Sedimentary Petrology 63, 683–693.
Törnqvist, T.E., Bridge, J.S., 2002. Spatial variation of overbank aggradation rate and its influence on avulsion frequency. Sedimentology 49, 891–905.
Törnqvist, T.E., Wallace, D.J., Storms, J.E.A., Wallinga, J., van Dam, R.L., Blaauw, M., Derksen, M.S., Klerks, C.J.W., Meijneken, C., Snijders, E.M.A., 2008. Mississippi Delta subsidence primarily caused by compaction of Holocene strata. Nature Geoscience 1, 173–176.
Tovey, N.K., Paul, M.A., 2002. Modelling self-weight consolidation in Holocene sediments. Bulletin of Engineering Geology and the Environment 61, 21–33.
Vos, P.C., Van Heeringen, R.M., 1997. Holocene geology and occupation history of the province of Zeeland (SW Netherlands). Mededelingen — Nederlands Instituut voor Toegepaste Geowetenschappen TNO 59, 5–109.
Wardenaar, E.C.P., 1987. A new hand tool for cutting peat profiles. Canadian Journal of Botany 65, 1772–1773.
Whittington, P.N., Price, J.S., 2006. The effects of water table draw-down (as a surrogate for climate change) on the hydrology of a fen peatland, Canada. Hydrological Processes 20, 3589–3600.